AFRL-RH-WP-TR-2022-0036

EXACERBATION OF TRAUMATIC BRAIN INJURY BY PSYCHOLOGICAL STRESS, HYPOBARIA, AND HOMOCYSTEINEMIA

Flaubert Tchantchou

University of Maryland, Baltimore

MARCH 2022
Final Report

AIR FORCE RESEARCH LABORATORY
711TH HUMAN PERFORMANCE WING,
AIRMAN SYSEMS DIRECTORATE,
WRIGHT-PATTERSON AIR FORCE BASE, OH 45433
AIR FORCE MATERIEL COMMAND
UNITED STATES AIR FORCE

NOTICE AND SIGNATURE PAGE

Using Government drawings, specifications, or other data included in this document for any purpose other than Government procurement does not in any way obligate the U.S. Government. The fact that the Government formulated or supplied the drawings, specifications, or other data does not license the holder or any other person or corporation; or convey any rights or permission to manufacture, use, or sell any patented invention that may relate to them.

This report was cleared for public release by the Air Force Research Laboratory Public Affairs Office and is available to the general public, including foreign nationals. Copies may be obtained from the Defense Technical Information Center (DTIC) (http://www.dtic.mil).

AFRL-RH-WP-TR-2022-0036 HAS BEEN REVIEWED AND IS APPROVED FOR PUBLICATION IN ACCORDANCE WITH ASSIGNED DISTRIBUTION STATEMENT.

//signature//

ALICIA BURKE, Program Manager
Program Manager
Product Development Branch
Airman Biosciences Division

//signature//

TERESA A. BEDFORD, Maj, USAF, NC, FNP-BC
Nurse Scientist, En Route Care
Product Development Branch
Airman Biosciences Division

This report is published in the interest of scientific and technical information exchange, and its publication does not constitute the Government's approval or disapproval of its ideas or findings

REPORT DOCUMENTATION PAGE

Form Approved
OMB No. 0704-0188

1. REPORT DATE *(DD-MM-YY)*	2. REPORT TYPE	3. DATES COVERED *(From - To)*
31-01-22	Final	01/23/2017 to 01/22/2022

4. TITLE AND SUBTITLE

Exacerbation of Traumatic Brain Injury by Psychological Stress,Hypobaria, and Homocysteinemia

5a. CONTRACT NUMBER

5b. GRANT NUMBER
FA8650-17-2-6H10

5c. PROGRAM ELEMENT NUMBER

6. AUTHOR(S)

*Flaubert Tchantchou

5d. PROJECT NUMBER

5e. TASK NUMBER

5f. WORK UNIT NUMBER
Legacy RHM

7. PERFORMING ORGANIZATION NAME(S) AND ADDRESS(ES)

*University of Maryland,Baltimore

8. PERFORMING ORGANIZATION REPORT NUMBER

9. SPONSORING/MONITORING AGENCY NAME(S) AND ADDRESS(ES)

Air Force Materiel Command
Air Force Research Laboratory
711th Human Performance Wing
Airman Systems Directorate
Airman Biosciences Division
Product Development Branch
Wright-Patterson AFB, OH 45433

10. SPONSORING/MONITORING AGENCY ACRONYM(S)
711 HPW/RHBA

11. SPONSORING/MONITORING AGENCY REPORT NUMBER(S)
AFRL-RH-WP-TR-2022-0036

12. DISTRIBUTION/AVAILABILITY STATEMENT
Distribution Statement A: Approved for public release.

13. SUPPLEMENTARY NOTES
AFRL-2022-2250, cleared 28 June 2022

14. ABSTRACT

United States military service members suffer substantial stress on the battlefield and during aeromedical evacuation. These stressful conditions result in systemic physiological changes that cause the neurotoxic accumulation of substances such as the non-proteinogenic amino acid homocysteine, which canbe deleterious to their health and exacerbate combat-related injuries, including traumatic brain injury (TBI). More than 300,000 service members sustained TBI during the Iraq and Afghanistan wars, with mild TBI (mTBI) representing more than 80% of all TBI cases. Despite longstanding scientific efforts in TBI research, the impact of stress on TBI pathophysiological outcomes is not elucidated. Male Sprague Dawley rats (300–350g; Envigo, CA) were exposed to environmental, physiological, or psychological stress paradigms before and after mTBI by controlled cortical impact. Stress exacerbated several TBI-associated pathological markers, including markers of oxidative stress, inflammation, blood-brain barrier disruption. Stress-induced exacerbation of mTBI pathological markers subsequently aggravated TBI-associated behavioral deficits, including working memory and anxiety-like behavior. Findings from this study expand the understanding for the development of effective therapeutic strategies to mitigate the impact stress sustained by U.S service members, resulting in improved TBI pathological outcomes

15. SUBJECT TERMS
Traumatic brain injury, Aeromedical evacuation, Hypypobaria exposure, hyperhomocysteinemia, psychological stress, oxidative stress, inflammation, blood-brain barrier disruption, behavioral deficits

16. SECURITY CLASSIFICATION OF:			17. LIMITATION OF ABSTRACT:	18. NUMBER OF PAGES	19a. NAME OF RESPONSIBLE PERSON (Monitor)
a. REPORT	b. ABSTRACT	c. THIS PAGE			Alicia Burke
Unclassified	Unclassified	Unclassified	SAR	53	19b. TELEPHONE NUMBER *(Include Area Code)* N/A

TABLE OF CONTENTS

1.0 BACKGROUND:

Military service members suffer substantial stress on the battlefieldand during aeromedical evacuation. These stressful conditions result in systemic physiological changes that cause the increased formation of toxic substances such as homocysteine (HCY), which canbe deleterious to their health and exacerbate combat-related injuries. Traumatic brain injury (TBI) is a significant public health problem and the signature injury of Operation Enduring Freedom and OperationIraqi Freedom, during which more than 300,000 service members were diagnosed with TBI. Despite longstanding efforts by the scientific community in TBI research, the pathophysiology of TBI and the contribution of physiologic and psychological stress to TBI outcomes are not clearly understood.

TBI victims in the Iraq and Afghanistan wars were often subjected to intercontinental aeromedical evacuation (AE) for advanced medical care within a few days after injury[1]. The cabin pressure during these flights is approximately equal to 8000 feet (ft) altitude. Goodman et al. (2011)[2] was the first to demonstrate that exposure to AE-relevant hypobaria within a few hours (hr) following TBI in mice worsens brain inflammation. Our Air Force-sponsored research found that exposure of adult male rats to 6 hours of these hypobaric conditions within three days following moderate TBI worsened neurobehavioral outcome, increased brain inflammation, and exacerbated cerebrovascular damage[3,4]. Importantly, aeromedical evacuation is associated with several stressors that could exacerbate TBI and other forms of injury. These stressors include hypobaria, vibration, acceleration/deceleration, and temperature variations, which alone or in combination may promote inflammation and oxidative stress[5]. Military activities, including stressful combat and regular combat practice and social behaviors among service members of excessive alcohol consumption and cigarette smoking[6,7], as well as hypobaria exposure at a high altitude starting at approximately 7500 ft, can result in hyperhomocysteinemia (HHCY) in humans[8–12]. Moreover, stress induction has been shown to cause HHCY in humans and rodents via exposure to psychological stressors[13], electric foot shock[14], or pro-oxidant dietary regimen[15,16]. Noticeably, HHCY increases the sensitivity of neurons and cerebral blood vessels to injury[17–19], exacerbates brain injury-induced cortical lesion volume[20], and is observed clinically in diseases and disorders ranging from Alzheimer's disease[21]to post-traumatic stress disorder[22].

Based on the pro-inflammatory and excitotoxic effects of TBI and HHCY, neuroprotective interventions targeting these mechanisms are needed. Omaveloxolone (RTA-408) is a triterpenoid and very potent activator of Nrf2 that has been tested in animal models and is pending FDA approval to treat the neurodegenerative disorder Friedreich ataxia[23]. Following its administration, RTA-408 inhibits Keap1 and prevents Nrf2 ubiquitination. Under stressful conditions, Nrf2 increasingly translocates into the nucleus, where it heterodimerizes with the small Maf (sMaf) protein. The heterodimer binds to the antioxidant response element (ARE) to upregulate the expression of glutathione metabolizing genes and other cytoprotective genes[24–26]. RTA-408 also increases the catalytic activity of crucial glutathione anabolizing enzymes, gamma-glutamyl-cysteine ligase (ɣGCL), and glutathione synthase (GS)[25,26], which facilitate homocysteine transsulfuration and promote increased glutathione biosynthesis, crucial to scavenging chronic stress and/or TBI-induced reactive radicals. Overall, RTA-408 is proven to attenuate oxidative stress by using synthesized glutathione to detoxify and scavenge free radical formation[25,27,28]. It also hasanti-inflammatory properties[24,29], can prevent cell death[25,27,28], and attenuate mitochondrial dysfunction[26–28], all of which are downstream effects of increased oxidative stress. RTA-408 demonstrated broad- spectrum therapeutic potential, suggests that it is an outstanding candidate to mitigate the impact of stress and treat TBI.

The objective of this study was to examine the effects of HHCY-induced stress on TBI secondary injury mechanism in a rodent model of controlled cortical impact (CCI)-induced TBI and its association with the deleterious impact of hypobaria exposure.

We hypothesize that (1) HHCY-induced stress before TBI worsens neurobehavioral and neuropathologic outcomes, which are further aggravated by exposure of rats to AE-relevant hypobaria at24 hr following injury.

We aimed to (1) Determine if pre-existing HHCY exacerbates TBI deficits in neurobehavioral outcomes, injury-induced lesion volume, and associated neuronal cell death, blood-brain barrier dysfunction, and inflammation. (2) Determine if exposure of sham or TBI rats to 6 hr hypobaria results in HHCY and neurobehavioral evidence of stress. (2) chronic psychological stress prior to injury increases serum HCY levels worsens the pathological and behavioral outcomes following TBI and hypobaria. (4) Determine folic acid or Omaveloxolne administered alone or in combination to protect against the effectsof pre-existing stress and hypobaria on TBI outcomes.

2.0. METHODS

2.1 Animals and housing

Male Sprague Dawley rats (300–350g; Envigo, CA) were used. They were housed in a temperature-controlled environment, maintained at 23 ± 2 degree celsius (ºC), with a 12h light/dark cycle, with access to food and water*ad libitum*. All animal procedures were approved by the University of Maryland, Baltimore, Animal Use and Care Committee, the USAF Animal Use Programs Office of Research Oversight & Compliance, andthe United States Army Medical Research and Development Command (USAMRMC). Animal Care and Use Review Office (ACURO) in compliance with all federal regulationsgoverning the protection of animals and research. Experimental groups consisted of 5-6 rats/group for immunohistochemistry or biochemical analyses and 10-12 for behavioral assessment. Animals were randomly assigned to groups.

2.2 Hyperhomocysteinemic rat model

Moderate HHCY was induced in rats by intraperitoneal injections of methionine (Sigma-Ulrich, MO) at 0.3g/kg once daily for seven days[30]. After surgery, methionine administration was continued until euthanasia on day 1, day 7, or 30 post-surgery. Body weight was measured immediately before the first methionine injection and weekly after that.

2.3 Restraint for stress Induction

Male Sprague Dawley rats (250-350grams (g)) were individually placed in a 21 cm by 6 cm diameter Broome rodent cylindrical restrainer (Harvard Apparatus, Cat # 52-0494) using the tail access line to put the animal in place. Each rat was maintained in its restrainer for 60 min daily. The procedure was repeated for 7 consecutive days prior to experimental brain injury induction by CCI method and continued until euthanasia on days 1, 7 or 31 post-injury.

2.4 Induction of Controlled Cortical Impact Injury

Mild traumatic brain injury (mTBI) was induced by CCI. All rats were under general anesthesia with 2.5 percent (%) isoflurane in 28% oxygen throughout the surgery. Rat body temperaturewas maintained at 37ºC using a heating pad coupled with a rectal probe. Following craniotomy over theleft parietal cortex, CCI

was performed with a stereotaxically positioned 4mm diameter piston tip. Impactinjury was done using an electromagnetically controlled impactor (Leica Biosystems, IL) with piston velocity set at 5m/sec and depth penetration of 1.5 millimeter (mm). The bone flap was replaced, the skin closed, and the anesthesia terminated. Sham-operated rats were also anesthetized, followed by craniotomy andreplacement of the bone flap in the absence of cortical impact.

2.5 Rat exposure to Hypobaria

At twenty-four hours post-surgery, rats were housed in cages with ad libitum food and water access and placed in a hypobaria chamber. A vacuum pump connected to the chamber was gradually adjustedto depressurize the chamber to 568 millimercury (mmHg), which is the ambient pressure at 8,000 ft. altitude. As previously reported, the chamber was kept normoxic (21% oxygen (O_2)) with supplemental O_2, were at a near- normal inspired oxygen level of 30%, the pulse oximetry (SpO_2) was 97.0% at a hypobaria level 8000 ft. Rats were maintained under these conditions for 6h, followed by depressurization every 15 minutes to sea level ambient pressure (757 mm Hg)[4]. As a control, other rats were placed in the chamber under normobaric conditions, equivalent to 80 ft., altitude, 21% O_2 for the same duration. Some sham or CCI rats (6/group)received intraperitoneal injections of 2-dihydroethidium (2-DHE) in 50% DMSO (6mg/kg) to track superoxide formation [31] during hypobaria or normobaria-exposure conditions, equivalent to 80 ft., altitude, 21% O_2 for the same duration. Some sham or CCI rats (6/group)received intraperitoneal injections of 2-dihydroethidium (2-DHE) in 50% DMSO (6mg/kg) to track superoxide formation[31] during hypobaria or normobaria-exposure.

2.6 Test compound preparation and administration

RTA-408 (> 99% purity) will be ordered from MedChemExpress, LLC (Monmouth Junction, NJ) and stock prepared in pharmaceutical grade DMSO. The stock was further diluted with corn oil and administered orally gavage) once daily at 4 milliliters per kilogram (mL/kg) of body weight (with a maximum gavage volume of 20ml/kg for rats) to achieve 20 mg/kg in 2% DMSO and 98% corn oil used as a vehicle.

2.7 Plasma homocysteine measurement

Homocysteine levels were measured in rat's plasma collected at days 1 and 7 post-surgery or at 2hand 24h post-hypobaria exposure. This was done using an enzymatic assay kit (BiooScientific, TX) following the manufacturer's instructions.

2.8 Evan's Blue preparation and via tail vein injection to rats and mice

Evan's Blue is a non-toxic dye used to assess blood-brain barrier permeability. Evan's Blue (Sigma Aldrich, MO) was dissolved at 2% (2mg/ml; w/v) in normal saline immediately before use and filtered through a 0.22 micromolar (μM) tissue culture filter. Two hours before euthanasia, rats were administered the 2% Evan's blue via lateral tail vein injection at 4 mL/kg. Two hours later, they were anesthetized and euthanized by exsanguination via transcardial flush with phosphate buffered saline (PBS). Brains were removed, submerged in formamide, and incubated at room temperature for 48 hours. The absorbance of the supernatant was measured at 620 nanometer (nm) using a Spectrophotometer (Fluster Optima, BMG LabTech, NC).

2.9 Measurements of oxidative stress markers in plasma and brain

2.9.1. Malondialdehyde measurements

Lipid peroxidation levels were determined by measuring the thiobarbituric acid reactive substance (TBARS) malondialdehyde (MDA) in rat plasma samples. The assay was performed using a kit (Cayman Chemical, MI) following the manufacturer's instructions.

2.9.2. Superoxide production

The formation of superoxide anion was monitored in rat brains during hypobaria using 2-dihydroethidium (Molecular Probes, OR), a fluorescent probe that incorporates between nucleic acid strands of superoxide producing cells[31]. DHE was dissolved in 50% DMSO and administered intraperitoneally at 6mg/kg immediately before hypobaria or normobaria exposure (n = 4/group). Rats were euthanized at two-hours post-exposure and brain removed, processed, sectioned, and preserved as described [32,33]. DHE incorporated cells were microscopically visualized with a 20x objective at 594 nmwavelength.

2.10 Measurements of reduced and oxidized plasma glutathione levels

Plasma samples were collected during euthanasia from sham or brain-injured rats at 2h, 24h, or 30days post-hypobaria or normobaria exposure. Total and oxidized glutathione concentration was measured using a colorimetric assay kit in rat plasma samples (n = 4/group) (Life Technologies Inc, MD).In brief, the assay used a colorimetric substrate that reacted with the free thiol group on glutathione to generate a highly colored product. Reduced glutathione concentration was the difference between total and oxidized plasma glutathione concentration measured separately, following the manufacturer's instructions.

2.11 Transcriptional analysis of glutathione metabolizing genes

Total RNA was extracted from snap-frozen samples of the ipsilateral prefrontal cortex, parietal cortex, and hippocampus from sham and CCI rats euthanized 2h post-hypobaria or normobaria- exposure (n=4/group). RNA extraction was done using the PureLink RNA Mini kit (Ambion/Life Technologies Inc., CA), following the manufacturer's instructions. Extracted RNA concentration was determined using a Spectrophotometer Nanodrop 2000C (Thermo Scientific, CA), and RNA tubes werestored immediately at -80ºC until used.

First, an Access RT-PCR system kit (Promega, WI) was used to amplify 2µg RNA and determine the optimal annealing temperature of primer sets designed for the quantitative amplification of glutathione metabolizing genes glutathione synthase (*GS)*, glutathione peroxidase 1 (*GPx-1)* and glutathione peroxidase 4 (*GPx-4),* as well as the housekeeping control gene glyceraldehyde 3-phosphate dehydrogenase (*GAPDH*) (Table 1).

Table 1: Presentation of forward (F) and reverse (R) primer sequences used for transcriptional analysis of glutathione metabolizing genes GS, GPX-1 and GPX-4. The table also shows the annealing temperature of these primers, their respective target amplicon size, and the mRNA sequence's access code from which each primer set was derived.

mRNA	Rat primer sequence (5'–3')	Annealing temp (ºF)	Amplicon (bp)	Access code
GS-F GS-R	ACA CAT CTT CAT TGC CCT CTC TCT ATG CCC ATC TAC CCT CTT	57	101	NM_012962.1
GPx-1-F GPx-1-R	GTT CCA GTG CGC AGA TAC A CCA GAT ACC AGG AAT GCC TTA G	57	111	NM_030826.4
GPx-4-F GPx-4-R	CCC ACT GTG GAA ATG GAT GA ACG CAG CCG TTC TTA TCA A	58.5	105	NM_017165.4
GAPDH-F GAPDH-R	CCC TTC ATT GAC CTC AAC TAC GAT GAC CAG CTT CCC ATT CT	55	102	NM_017008.4

Quantitative reverse transcriptase-polymerase chain reaction (Q-RT-PCR) was using thePower SYBR Green RNA-to-CT 1-Step kit(Applied Biosystem, MA). In brief, a complete RT-PCR mix containing 150 nM of primer (IDT, CA) that yielded the best annealing temperature for the respective GS, GPx-1, or GPx-4 gene of interestand GAPDH control was mixed with approximately 15µg of individual RNA template and placed in a 96 wells plate. Q-RT-PCR test of samples in the 96 wells plate was run in a QuantStudio-3 machine (Applied Biosystem, MA) for a total of 35 cycles after reverse transcriptase reaction at 48ºC for 30 min and enzyme activation at 95ºC for 10 min (n = 4/group). Each of the 35 Q-PCR cycles consisted of 15-sec denaturation at 95 ºC and 1min annealing/extension at the temperature noted in t able 1. Each sample was run in triplicate for the target genes GS, Gpx-1, or GPx-4 and duplicated for the reference gene, the glyceraldehyde-3-phosphate dehydrogenase (GAPDH). At the end of the run, the amplification of a single gene product was verified by the presence of a single peak in the melting curve analysis. Normalized cycle threshold (ΔCt) values were obtained bysubtracting the Ct of the reference gene from that of each of the target genes. The double delta Ct (ΔΔCt) for each target gene was determined by deducting the mean ΔCt of the target gene in the sham normobaric group from the ΔCt of the respective target gene. The fold-change of each target gene compared to the normobaric sham group was calculated as $2^{-\Delta\Delta Ct}$.

2.12 Lesion volume assessment

Hematoxylin and eosin (Sigma, MO) stained brain sections were dehydrated, cleared and mounted for lesion volume estimation. Injury lesion volume was quantified from eight sections corresponding to every 24 serial expanding from bregma 1.05 to -6.30 to cover the complete lesion area (n = 5/group). Quantification was done using the Cavalieri estimator method of unbiased stereology using the stereo-investigator software (MBF Biosciences, VT). The contusion region (impact-induced damaged region resulting in tissue loss) and penumbra region (the pathologically affected region around impact-induced lesion that could be salvaged with an effective therapeutic intervention) were outlined in the ipsilateral hemisphere of all sections with a grid spacing of 100 µm, and the injury lesion volume was determined and expressed in mm[334,35].

2.13 Histological analysis

2.13.1. Immuno-fluorescence staining

Brain sections were co-stained for the expression of the oxidative stress marker nitrotyrosine and the neuron-specific neuronal nuclear antigen (NeuN) or the pro-inflammatory marker the intracellular adhesion molecule 1 (ICAM-1) and the blood vessel marker laminin as previously described [36–38]. Briefly, free-floating sections were rinsed in phosphate-buffered saline (PBS) and blocked in 1% horse serum in PBS containing 0.3% Triton X for 1 h. Sections were then transferred in an antibody mixture containing rabbit anti-nitrotyrosine polyclonal antibody (1:2500; Sigma, MO) and mouse anti-NeuN monoclonal antibody clone, A60 (1:1500; Millipore/Sigma, MO) or goat anti-ICAM-1 polyclonal antibody (1:2000; Santa Cruz, CA) and rabbit anti-laminin polyclonal antibody (1:5000; Abcam, MA) and incubated at 4 °Covernight. Sections were washed in PBS and incubated in a mixture of corresponding secondary antibodies Alexa Fluor 488 or Alexa Fluor 594 (1:2000; Invitrogen, NY), for 1 h at room temperature. Sections were washed with PBS, counterstained with 4,6-diamidino-2-phenylindole (DAPI), and mounted with an anti-fade mounting medium (Vector Labs, CA).

2.13.2. Nickel DAB immunostaining

Brain sections were antibody-stained for the expression of the inflammatory marker CD-68 or the endothelial cell marker, the Von Willebrand Factor (vWF) protein, using nickel DAB staining. In brief, free-

floating sections were rinsed in PBS, blocked with 1% horse serum, and incubated in mouse anti-CD-68 monoclonal antibody (1:100k; Thermo-Fisher, MA) anti-vWF (1/2000; Abcam, MA) overnight at 4 °C. Sections were washed and incubated for 1-hr at room temperature in biotinylated horse anti-mouse secondary antibody (1/600 or 1/2000 respectively; Vector Laboratories Inc., CA), followed by incubation in Vestastain solution and nickel DAB and PBS washes. Sections were then mounted with DPX (Sigma, MO).

2.13.3. Transmission Electron microscopy

Four brain sections (40µm) from NHCY-sham animals were stained with hematoxylin and eosin (Sigma,MO) to locate the hippocampal fissure, highly vascularized to present endothelial cells. Stained brain sections were dehydrated, cleared, and mounted with DPX (Sigma, MO).
For the transmission Electron microscopy, the hippocampal dentate gyrus upper blade (40µm) containingthe hippocampal fissure was micro-dissected, fixed, dehydrated, and embedded in Epoxy resin following standard procedures. 70µm ultrathin sections were collected and imaged with a Transmission Electron Microscope (Technai T12, ThermoFisher) at 80 KeV using an AMT digital camera to capture the blood vessel ultrastructure.

2.14 Western blot analysis

Western blotting was performed to assess the expression of 4-hydroxy-2-nonenal (4-HNE), Zona occludens (ZO-1), occludin, alpha-2 spectrin protein, B-cell CLL/lymphoma 2-associated X protein (BAX), extracellular signal-regulated kinases 1 and 2 (ERK1/2), phosphorylated ERK1/2 (pERK1/2), serine/threonine kinase(AKT), phosphorylated serine/threonine kinase (pAKT), and beta actin (β-actin) (loading control) in the homogenates-supernatants of S1/S2 cortical brain region. Theexpression of thrombin and transferrin (loading control) was measured in freeze-thawed plasma. All brainhomogenates-supernatants were processed for electrophoresis as previously described [32,37–39]. Plasma samples were diluted 1:4 in PBS, and 25µg of total protein in brain homogenate-supernatants or plasmawere separated by electrophoresis on 4–12% SDS-polyacrylamide gels (Invitrogen, CA), then transferredto a nitrocellulose membrane (Sigma, MO). Membranes were blocked with 5% non-fat milk in Tris- buffered saline with 0.1% Tween-20 (TBST) and incubated overnight at 4 °C in rabbit polyclonalantibodies against occludin (1:2000; Abcam, MA), 4-HNE (1:4000; Millipore, MA), thrombin (1:2000; Abcam, MA) or transferrin (1:6000; Abcam, MA); a rat anti-ZO-1 monoclonal antibody (1:400, Millipore,MA) α-ii spectrin (1:3000; Invitrogen/ThermoFisher Scientific, NY), BAX, ERK,1/2, pERK1/2, AKT, pAKT(1:1000; Cell Signaling Technology, MA) or a mouse anti-β-actin (1:4000; Sigma, MO). Blots were washed in Tris-buffered saline with 0.1% Tween-20 and incubated for 1 h at room temperature with corresponding HRP-conjugated secondary antibodies (1:5000; Millipore, MA). Horseradish peroxidase- labeled proteins were detected by enhanced chemiluminescence (ECL, Thermo Scientific, IL), and protein bands were visualized using a digital blot scanner (LI-COR, NE).

2.15 Behavioral testing

All behavioral tests were performed at time points described in the experimental time

2.15.1. Beam Walk test

This test was performed to assess fine motor movements, as previously described[39,40]. Briefly, animals were trained to walk on a 1.5 mm wooden beam for three consecutive days, and baseline data determining the number of foot faults over a total of fifty steps were collected on day 4[39]. Test to assessthe effect of hypobaria-exposure on fine motor movement in sham and CCI rats overtime was performedon days 3, 9, 16, and 30 post-surgery.

2.15.2. Y Maze test

Animals were assessed for hippocampus-dependent working memory performance using the Continuous Spontaneous Alternation method[41] on days 1, 7, 14, and 28 post-surgery. The test used a Y-shaped device with arm dimensions of 35cm long, 5cm wide, and 15cm tall and was performed as we previously described[32,38,42]. In brief, animals were individually placed at the center of the Y maze and allowed to explore the three arms for 5 min. The sequence and number of each arm entry were tracked with a video camera and recorded for 5 min. An arm visit referred to the animal moving all four paws into the arm, and each alternation was defined as a consecutive entry in three different arms. The percent spontaneous alternation is calculated based on the formula: total number of alternations/(total number of arm entries – 2)[43].

2.15.3. Elevated Plus Maze test

The Elevated Plus maze was used to assess rats for anxiety-like behavior on days 2, 8, 15, and 29 post-surgery using a Plus-sign shape device as previously described [32,38]. Briefly, rats were individually placedin the central area of the device and allowed to explore the maze for 10 min. Animal movements were analyzed by an overhead camera, and data was collected and analyzed by Any-Maze software (SD instrument, CA) to provide several behavioral parameters, including the time spent in open arms. Anxiety-like behavior was interpreted as inversely proportional to the time an animal spent in the open arms.

2.16 Quantitation and statistical analysis

The stereo-investor software (MBF Biosciences) was used to quantify nitrotyrosine immuno-positive cells and for injury lesion volume measurement. For both measurements, a total of 6 sections were obtained to cover the entire impact region, − 1.60 mm to − 6.3 mm from Bergman, corresponding to every12 serial sections for each brain. For the quantification of nitrotyrosine immuno-reactive cells, the opticalfractionator method of stereology was employed to count these cells in the corpus callosum of 40 micrometer (μM) thick sections. Using a grid spacing of 75μm × 75μm in the *x* and *y*-axis and guard zones of 2μm at the top and bottom of each section, immuno-positive cell-bodies were counted. The total number of nitrotyrosine positive cells in the volume of interest was automatically determined and expressed as cells/$mm^{3.}$

Image J software (NIH) was used to determine the percent area covered by DHE incorporated cells,CD-68, ICAM-1, or vWF immune-reactivity. To achieve that, 30 microscopic fields of each serial sectionfrom DHE or saline-injected rats were captured with an SRS fractionator of the stereo-investigator software (MBF Biosciences, VT). Each image was optically segmented with a threshold greyscale valueof 0.3 μm, and the percent DHE-positive area was automatically measured. The mean of all DHE positivemicroscopic fields was determined.

Statistical analyses were performed using GraphPad InStat-3 software (GraphPad Software, Inc., CA). Data from biochemical and histological tests were analyzed using One-Way ANOVA and repeated ANOVA for behavioral data. Both tests were coupled to the Tukey-Kramer post-test to comparedifferences among the various groups. Results were expressed as mean ± standard error of the mean (SEM). Statistical significance was defined as $p < 0.05$. The individuals performing histologic, biochemical, and behavioral assays were blinded to animal group identifications, using codes revealed after data collection.

3.0 RESULTS:

3.1 Methionine induces HHCY and influence of hypobaria exposure and restraint-induced stress on plasma homocysteine levels

To determine if methionine (Met) injections increased homocysteine (HCY) as reported in the literature[22], animals were given Met injections for 7 days (groups CCI or Sham surgery) and plasma HCY levels measured. These Met injections resulted in a six-fold increase in HCY levels at both days-1 and 7 post-injury (pi) (Fig. 1A). Plasma HCY concentrations in the Met injection groups were 39.5 ± 5.52 µM (day 1 pi, sham) and 37.7 ± 10.1 µM (day-1 pi, CCI) compared to 5.9 ± 3.32 µM (day 1 pi, sham) and 4.5 ± 4.2 µM (day 1 pi, CCI) for saline injected rats ($p < 0.001$; 1A). This level of Met is considered clinically moderate [36,37]. This HCY level was maintained by continuous daily methionine injections.

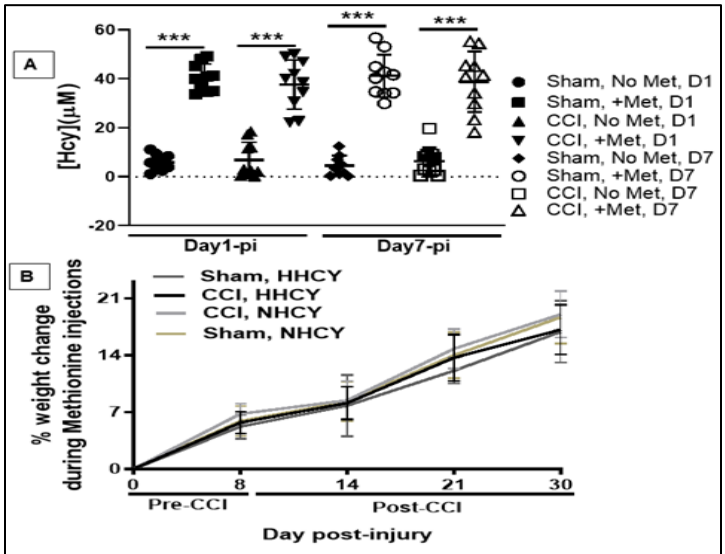

Figure 1. Hyperhomocysteinemia induction by systemic methionine: Methionine injections, once daily, to CCI and sham-operated rats at 300mg/kg sustained 6-fold increase in homocysteine levels in both groups compared to saline injected rats (n = 10/group; ***$p < 0.001$). (B) Hyperhomocysteinemia had no significant effect on the percent weight gain on both sham-operated and CCI rats (n = 10/group; $p > 0.05$).

As HHCY could alter post-surgical feeding and recovery, the weight of animals was measured on days 8 and 14, 21 and 30 post-surgery. The presence of moderate chronic HHCY did not alter rat's post-surgery weight gain progression. HHCY as well as normorhomocysteinemic (NHCY) sham and CCI rats weight gain ranged from 5.2% - 6.8% with no differences between sham, CCI, methionine or saline injections ($p=0.2$; Figure 1B).

To determine the effect of acute hypobaria-exposure on HCY metabolism, we measured plasma HCY levels at 2h and 24h after 6h of 8000ft hypobaria-exposure using normobaria-exposure as control. We found that mTBI alone significantly reduced plasma HCY levels in normobaria-rats after 2h after exposure, 1.41 ± 0.723 µM, compared to normobaria-shams, 4.32 ± 0.431 µM ($Q = 4.31$, $p < 0.05$). At the same 2h time point, HCY levels were further reduced or undetectable in the plasma of TBI rats exposed to hypobaria to 0.27 ± 0.28 µM and were significantly lower than levels in normobaric (3.12± 0.63 µM) and hypobaric (4.32 ± 0.431 µM) shams ($Q = 0,41$, $p < 0.05$; $Q = 5.88$, $p < 0.01$ respectively). HCY levels in CCI-hypobaria animals were still significantly reduced 24h after hypobaric 1.85 ± 0.63 µM compared to normobaric shams ($Q = 4.23$, $p < 0.05$). Hypobaria-exposure also caused a non-significant decrease in HCY levels among non-TBI sham rats with levels of 3.12± 0.63 µM at 2h post-exposure and 2.07 ± 0.52 µM at 24h post-exposure compared to normobaria-shams 4.32 ± 0.431 µM ($p > 0.05$).

The impact of restraint-induced chronic psychological stress on HCY metabolism was determined by measuring plasma HCY levels in non-restraint (NRst) and restraint (Rst) sham and brain-injured rats on days 1 and 7 pi. Results found on day 1 pi, 1.8 and 2-folds increases in HCY levels in Rst-sham (10.44 ± 2.47 µM) and Rst-CCI (12.82 ± 4.17µM) compared respectively to NRst-sham (5.44 ± 2.23µM) and NRst-CCI (5.95 ± 1.37µM); $n = 8$, $p < 0.01$. Similar changes were observed on day 7 pi. Restraint-CPS caused a sustained increase in HCY in sham and CCI rats, among whom 50-60% presented HHCY (HHCY), clinical defined as plasma HCY ≥ 15 µM[36,37].

3.2 Hypobaria-induced increases oxidized glutathione

We measured reduced and oxidized glutathione levels in that plasma. This showed that hypobaria-exposure caused a modest increase in oxidized glutathione in sham rats at 2h post-exposure (1.25 ± 0.23 μM) compared to normobaria-shams (0.76 ± 0.19 μM; $p > 0.05$;). TBI alone had no effect on glutathione oxidation among normobaria-rats at 2h post-exposure (0.723 ± 0.158 μM) compared to normobaria-shams (0.76 ± 0.19 μM; $Q = 0.56$, $p > 0.05$;). However, the combination of TBI and hypobaria significantly increased plasma oxidized glutathione to 1.998 ± 0.296 μM compared to CCI-normobaria and CCI-hypobaria 24-h and 30 days post-surgery ($Q = 4.41$, $p < 0.05$ and $Q = 9.23$, $p < 0.01$ respectively).

The ratio of oxidized to reduced glutathione is an important metric of the metabolic impact of TBI and hypobaria on glutathione metabolism. When we assessed the ratio of oxidized to reduced glutathione, we found that hypobaria-exposure substantially enhanced oxidized glutathione over reduced glutathione in both sham and CCI rats resulting in 1.57 ± 0.202 and 2.38 ± 0.323-ratios respectively, compared to 0.741 ± 0.164 μM and 0.99 ± 0.22 μM for normobaria-sham and CCI rats ($p < 0.05$). This ratio decreased significantly overtime at 24h and 30-days ($Q = 4.61$, $p < 0.05$ and $Q = 6.79$, $p < 0.01$respectively) post-exposure in a time-dependent manner. The elevation of oxidized glutathione implies increased free radical scavenging through glutathione oxidation [38], which could activate the endogenous glutathione oxidizing metabolic pathways.

3.3 Hypobaria induces upregulation of glutathione metabolizing genes

We examined the transcriptional profile GS, GPx-1, and GPx-4 in three regions of the ipsilateral hemisphere, the prefrontal cortex, parietal cortex, and hippocampus, at 2h post-exposure, to determine how their expression responds to hypobaria-exposure. All results are presented in table 2.

Table 2: Presentation of transcriptional analysis results of glutathione metabolizing genes GS, GPX-1) and GPX-4 in the prefrontal cortex, the parietal cortex of shams, and CCI rats exposed to normobaric or hypobaric conditions. These results represent the fold expression change of each of these genes in different experimental groups compared to normobaric-shams used as control.

	Prefrontal cortex			Parietal cortex			Hippocampus		
Study groups	GS	GPx-1	GPx-4	GS	GPx-1	GPx-4	GS	GPx-1	GPx-4
Sham, NB	1 ± 0.086	1 ± 0.045	1 ± 0.05	1 ± 0.059	1 ± 0.3	1 ± 0.021	1 ± 0.034	1 ± 0.124	1 ± 0.138
Sham, HB	1.33 ± 0.24	1.35 ± 0.19	1.28 ± 0.137	1.2 ± 0.2	1.45 ± 0.03	1.33 ± 0.18	2.25 ± 0.14	1.5 ± 0.05	1.84 ± 0.04
CCI, NB	7.23 ± 0.53	11.16 ± 0.56	4.5 ± 0.32	0.95 ± 0.05	1.65 ± 0.1	1.26 ± 0.14	1.12 ± 0.005	1.54 ± 0.06	1.62 ± 0.12
CCI, HB	8.43 ± 1.51	14.5 ± 0.58	3.68 ± 0.95	3.33 ± 0.26	4.04 ± 0.6	1.46 ± 0.15	1.12 ± 0.02	2.99 ± 1.36	1.58 ± 0.023

These results show a heterogeneous expression pattern in different brain regions**.** In the prefrontal cortex, the expression of all three genes was enhanced by the cortical imp (PTC)act-induced brain injury (Table 2; $Q = 4.51$, $p < 0.05$; $Q = 6.90$, $p < 0.01$; $Q = 9.83$, $p < 0.001$) with no significant effect of hypobaria-exposure only on the expression compared to normobaria-shams. In contrast, the combination of cortical brain injury and hypobaria-exposure upregulated the expression of GS and GPX-1 in the parietal cortex compared to normobaric brain-injured rats as well as hypobaric and normobaric shams (Table 2; $Q = 6.26$, $p < 0.01$). There was no significant change in GPX-4 expression in the parietal cortex of rats in any group (Table 2; $p > 0.05$). In the hippocampus, GS expression was significantly upregulated by hypobaria alone in shams compared to other groups (Table 2; $Q = 15.32$, $p < 0.001$). Similar to the parietal cortex, hypobaria or CCI only increased the expression of GPX-1 in the hippocampus and the combination of both resulted in more upregulation, although all are non-significant (Table 2; $p > 0.05$). The expression of GPX-4 in the hippocampus was increased by injury or hypobaria alone, and no additional effect of the two combined (Table 2; $Q = 7.1$, $p < 0.01$; $Q = 9.96$, $p < 0.001$). In summary, the expression of glutathione metabolizing genes was differentially affected by brain injury, hypobaria, or by the combination of both factors, dependent on the targeted brain region.

3.4 Hypobaric conditions increase oxidative stress

The biochemical markers above indicate that there may be considerable oxidative stress causing a compensatory reduction in HCY and elevation in the processing of glutathione antioxidant systems. Consistent with this conjecture, we found that TBI caused a non-significant 12.3 ± 5.23% increase in plasma malondialdehyde levels in normobaria-CCI rats at 2h post-exposure compared to normobaria-shams ($p > 0.05$). In addition to the modest increase in TBI, when combined with hypobaria-exposure, there was a significant increase in MDA formation of 55.38 ± 10.5% over baseline ($Q = 6.83$, $p < 0.01$).

Although there is generally a good correlation between blood and brain biomarkers in TBI studies [39], these measures of oxidative stress do not give information on where in the body they originate. To verify which brain regions were impacted by hypobaria induced free radical formation during hypobaria exposure, we used 2-DHE for in vivo tracking of superoxide production in brain cells (Figure 2A) and compared conditions by measuring the percentage of pixels in defined brain regions that are 2-DHE positive. There was significant increase in 2-DHE incorporated cells in normobaria-CCI rats (2.42 ± 0.18% area covered) compared to normobaria-shams (1.02 ± 0.16%; Figure 2B; $Q = 0.46$, $p < 0.05$). Hypobaria-exposure alone did not cause a significant change in superoxide production in sham rats resulting in 1.59 ± 0.18% versus normobaric-shams (1.02 ± 0.16%; Figure 2B; $p > 0.05$). However, in the presence of hypobaria with CCI, there was a marked increase in 2-DHE positive cells present with five times the area compared to sham (TBI/CCI 4.58 ± 0.62% of the brain region; Figure 5B; $Q = 0.68$, $p < 0.01$) and normobaria-CCI rats ($Q = 0.46$, $p < 0.05$). Thus, hypobaria-exposure exacerbates TBI associated oxidative stress.

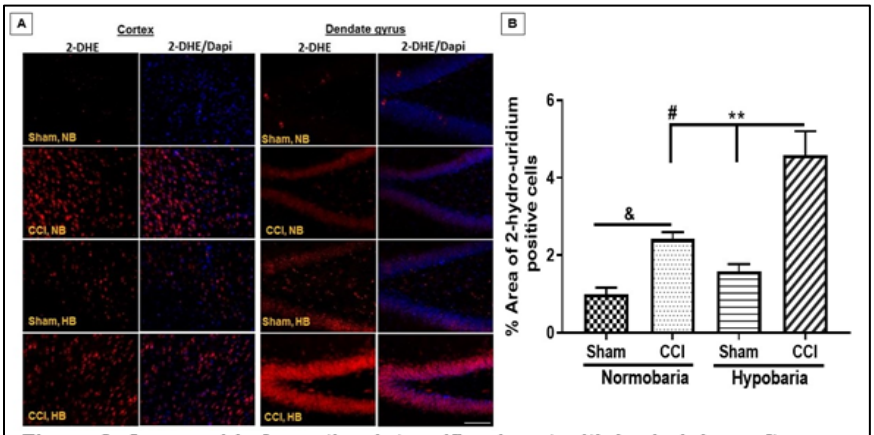

Figure 2. Superoxide formation intensifies in rat with brain injury after hypobaria exposure. Representative microscopic images showing 2-DHE incorporation in superoxide producing cells in the injury penumbra region and the hippocampus dentate gyrus. Quantitation of the %area of 2-DHE positive cells **(B)** indicates that brain injury alone caused a significantly increased superoxide formation (n = 4; &$p < 0.05$) and this was aggravated by hypobaria-exposure (n = 4; #$p < 0.05$, **$p < 0.01$). The scale bar is 100 µm.

3.5 TBI lesion volume was not significantly affected by hypobaria exposure

To assess the effect of hypobaria-exposure on brain injury lesion, we used the Cavalieri method of unbiased stereology to measure injury-induced lesion volume at 2h and 24h post-exposure. At 2h post-exposure, impact-induced injury lesion volume was approximately the same between normobaric, 6.56 ± 2.25 mm^3, and hypobaric-CCI rats, 7.09 ± 1.42 mm^3 ($p > 0.05$). But at 24h post-exposure, corresponding to 48h post-surgery, brain injury lesion volume presented a non-significant increase following hypobaria exposure, 13.68 ± 3.05 mm^3 compared to 6.78 ± 2.48 mm^3 among normobaric-rats ($p > 0.05$). This suggests that hypobaria exposure has no acute negative impact on TBI brain tissue loss.

3.6 Hypobaria exposure increases anxiety-like behavior in rats with mild TBI

Next, we wanted to determine whether hypobaria exposure following mTBI in animals exacerbates behavioral deficits. We assessed the effect of hypobaria-exposure on anxiety-like behavior usually associated with TBI-related psychiatric impairment such as posttraumatic stress disorder[40,41]. Anxiety was assessed with a standard elevated plus-maze in which reduced time spent in the open arms of the maze is interpreted as elevated anxiety-like behavior. As a control, fine motor behaviors classically associated with cerebellar function, a brain region removed from the injury site, were not significantly affected as assessed by the Beam Walk test. On day 2 post-exposure, which is an early time point when changes due to hypobaria are mostly likely detectable, normobaric sham and CCI rats respectively made 1.28 ± 0.98 and 1.87 ± 0.62-foot faults over 50 steps. In comparison, hypobaric sham and CCI rats made 1.39 ± 0.75 and 1.77 ± 1.02 foot faults ($p > 0.05$, all compared to normobaric shams). However, brain-injured rats exposed to hypobaria spent significantly less time in the open arms of Plus maze on days 2 and 8 post-injury, indicative of increased anxiety compared to normobaria-shams. These animals spent 48.21 ± 10.74 s and 94.08 ± 21.49 s in the open arms of the Plus maze on days 2 and 8 respectively versus 133.04 ± 25.28 s and 241.82 ± 29.12 s for normobaria-shams (Figure 3; $Q = 5.21$ and 5.58 respectively; $p < 0.05$). To a lesser extent, hypobaria-sham and normobaria-CCI rats also exhibited some deficits in anxiety-like behavior on days 2 and 8 post-surgery (Figure 3; $Q < 4.96$ thresholds for significance; $p > 0.05$), compared to normobaria-shams. After 8 days, rats in all groups recovered from this deficit and exhibited Plus maze performance close to normobaric-shams.

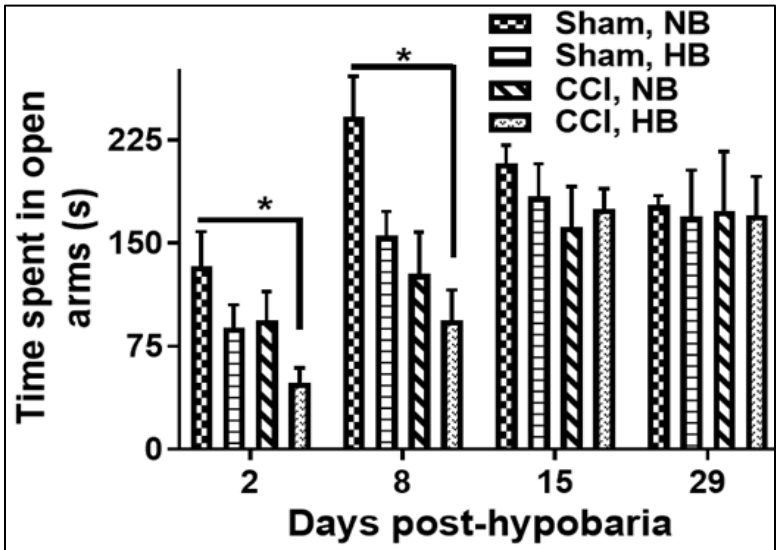

Figure 3. Traumatic brain injury-induced anxiety-like behavior is aggravated by hypobaria exposure. Graph depicting the time spent by rats in the open arms of the Elevated Plus maze. Both brain injury and hypobaria alone caused a non-significant in anxiety-like behavior. The combination of mTBI and hypobaria significantly increased anxiety-like behavior on days 2 and 8 post-surgery compared to normobaric-shams (n = 8/group; *$p < 0.05$). Two and four weeks post-HB, this behavioral deficit was resolved, and rats in all groups spent closely the same time in the plus-maze open arms ($p > 0.05$).

3.7 HHCY exacerbates traumatic brain injury induced oxidative stress

Chronic moderate HHCY is associated with oxidative stress in humans[42,43] and mTBI is also associated with elevated oxidative stress in multiple animal disease models [44,45]. Therefore, we hypothesized that each condition alone would elevate markers of oxidative stress and that the combination of HHCY and CCI would yield greater levels of oxidative stress. To test this, the ipsilateral hemisphere levels of 4-HNE, a marker of oxidative modifications, were measured in the cortex. Western blot analysis showed a significant increase of 51 ± 14% ($p < 0.05$; Figure 4A-B) in 4-HNE levels in the S1/S2 cortex of HHCY-sham compared to NHCY-rats at day 7-pi. HHCY also dramatically increased 4-HNE expression was exacerbated in hyperhomocysteinemic-CCI rats both at day 1 and 7-pi showing 76 ± 24% and 57 ± 15% respectively ($p < 0.01$; Figure 4A-B).

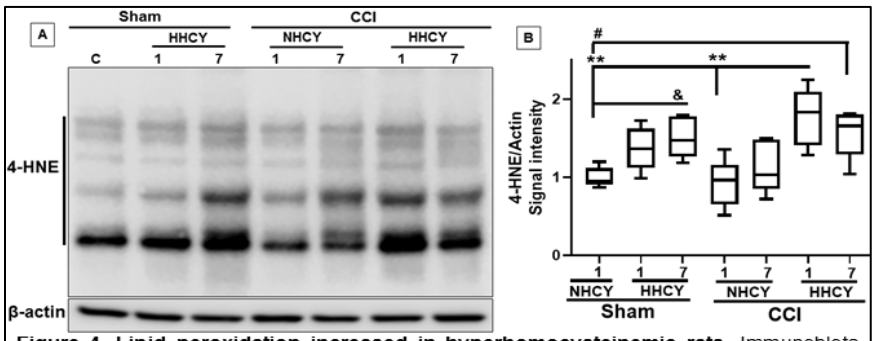

Figure 4. Lipid peroxidation increased in hyperhomocysteinemic rats. Immunoblots illustrating the expression of 4-hydroxynonal in the S1/S2 cortex at days 1 and 7 post-surgery. (B) Quantification of protein bands indicated that 4-HNE expression was significantly increased in the cortex HHCY-CCI rats than NHCY-sham and CCI at days 1 or 7 post-surgery (n = 5; #,&$p < 0.05$ and **$p < 0.01$). Changes in 4-HNE expression was also significantly greater in the cortex HHCY-sham rats than NHCY-shams.

Following the observation of HHCY induced oxidative stress within the ipsilateral injured cortex, we hypothesized that there may also be oxidative stress responses along the major white matter tracts from the injured cortex. To examine this, we stained for 3-nitrotyrosine and examined nitrotyrosine positive cells in the corpus callosum. Nitrotyrosine was elevated in astrocyte-like cells in the corpus callosum (figure 3) of saline-injected as well as HHCY-CCI rats. These astrocyte-like cells had star-like appearance with multiple processes deriving from the soma. To quantify these observations, cells in the corpus callosum were counted using optical fractionator. Nitrotyrosine positive cells in the corpus callosum of HHCY-sham rats was significantly greater, 5,600 ± 1300cells/mm^3 compared to NHCY-shams with 456 ± 195 cells/mm^3 ($p < 0.05$). We also found an average of 11,400 ± 3900 cells/mm^3 in the corpus callosum of HHCY-CCI rats compared to 7500 ± 2400 cells/mm^3 in NHCY-CCI rats ($p < 0.05$). Interestingly, there was not significant difference between the number nitrotyrosine positive cells in the corpus callosum of HHCY-sham vs NHCY-CCI rats ($P > 0.05$) suggesting HHCY might be as oxidatively stressful to the corpus callosum of sham as mTBI rats. The data indicate that the combination HHCY-CCI increased glial oxidative stress in the corpus callosum to a level higher than HHCY or CCI alone.

3.8 Increased homocysteine levels worsened traumatic brain injury associated blood brain barrier dysfunction

HHCY has been implicated in vascular stress and pathological changes in multiple organ systems[46,47]. To assess vascular changes in the brain, the effect of HHCY on blood brain barrier (BBB) function was assessed by examining the expression levels of tight junction proteins ZO-1 and occludin and Evans blue extravasation test. ZO-1 expression was reduced by 42 ± 16% in the cortex of HHCY-shams at day 1 post-surgery compared to NHCY-shams ($p < 0.05$; figure 4A, B). CCI alone also decreased the expression of ZO-1, consistent with our previous reports on BBB disruption in blast TBI models[24,30]. At day 7-pi, ZO-1 levels were 63 ± 7% lower in the cortex of CCI injured NHCY-rats compared to NHCY-shams ($p < 0.001$; figure 4A, B). The reduction in ZO-1 in CCI was further exacerbated by HHCY, resulting in 70 ± 8% decrease in expression at days 7-pi ($p < 0.001$; Figure 4A, B).

In contrast, occludin cortical expression in NHCY-sham and CCI rats were unchanged. HHCY reduced expression of occluding in both sham and CCI to a similar magnitude. Occludin in HHCY-rats was 30 ± 9% lower at day-1 compared to levels in NHCY-shams and CCI rats ($p < 0.05$; figure 4-A, C) and occludin levels were reduced by 29 ± 13 % and 33 ± 17% at day 7-pi in HHCY-sham and CCI rat cortex compared to NHCY-CCI ($p < 0.05$, figure 4A, C). This shows that HHCY has a significant effect on reducing occludin, but CCI does no further effect in suppressing its expression.

Since we observed that HHCY reduces both ZO-1 and occludin expression, we hypothesized that the BBB would become leaky from the disruption of these tight junction proteins. To quantify BBB permeability, we used the classic Evans blue dye extravasation test [31,48]. This is performed by injecting Evans blue dye into the blood stream and then quantifying the amount of Evans blue dye present in the brain parenchyma. Evans blue extravasation was enhanced by both HHCY and CCI brain injury. Evans blue presence was significantly greater in the ipsilateral and contralateral hemispheres of HHCY-sham rats at day 1 post-surgery (4.04 ± 0.06ηg/mg) compared to NHCY-shams (2.06 ± 0.46ηg/mg; figure 5A, B; $p < 0.05$). CCI only animals showed BBB disruption only in the ipsilateral cortex, however, HHCY enhanced Evans blue extravasation both the ipsilateral and contralateral cortex, with the greatest extravasation present in the combination of CCI plus HHCY.

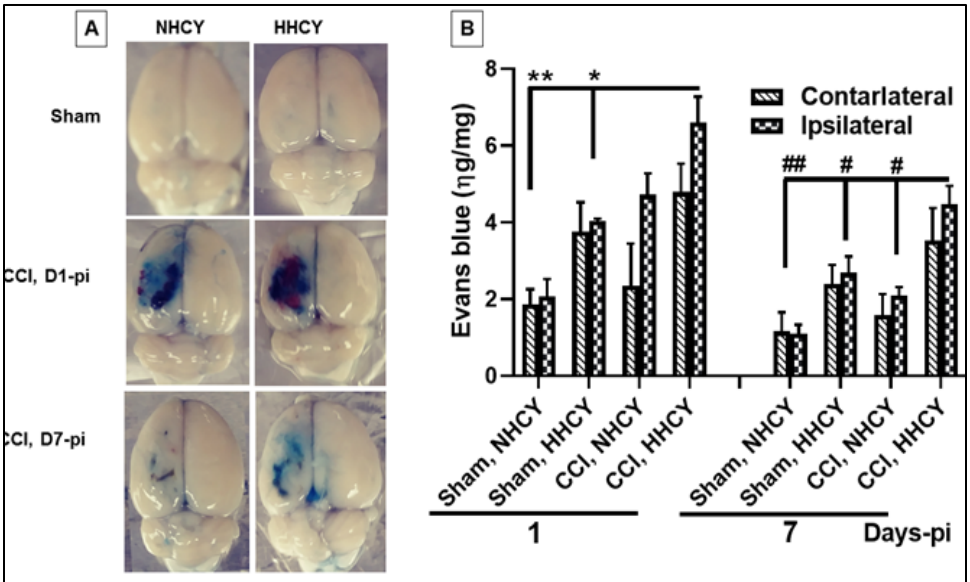

Figure 5. Hyperhomocysteinemia exacerbates Evans blue extravasation in CCI-injured rat brains. (A) Representative brain images from nhcy and hhcy-sham and -CCI rats injected with Evans blue solution at days 1 or 7 post-surgery. (B) Quantitation of Evans blue in formamide showed a significant increase in Evans blue extravasation in the ipsilateral hemisphere of NHCY-CCI rats at day 1 post-injury (n = 5/group; *$p < 0.05$ and **$p < 0.01$). This effect was aggravated by homocysteine accumulation. Despite the reduction of the amount of HCY in the brain parenchyma, the detrimental effect of HHCY persisted, till day 7 post-surgery (n = 5/group; #$p < 0.05$ and ##$p < 0.01$).

Although tight junction protein expression is depressed over 7 days, there could be restoration of BBB function overtime post-injury. Indeed, at day 7-pi, CCI-induced Evans extravasation in the ipsilateral hemisphere was significantly resolved resulting in 55% decrease of dye presence compared to day 1-pi (figure 5A, B; $p < 0.01$). However, the effect of HHCY persisted with 4.48 ± 0.94ηg/mg HHCY-CCI rat's ipsilateral hemisphere and two-fold greater than in NHCY-CCI rats ($p < 0.05$). Taken together, these data show that HHCY disrupts BBB function in sham and yields further disruption to BBB function following CCI induced mTBI (6.6 ± 1.36ηg/mg).

3.9 Homocysteine toxicity potentiates the expression of blood clotting associated proteins following traumatic brain injury

HHCY disruption of the BBB function in the brain and vascular function in other organs, there could be a concomitant change in blood coagulation proteins. Thus, we examined the effect of HCY accumulation on

blood by measuring blood clotting-associated markers such as von Willebrand factor, an endothelial and pro-coagulation marker[49,50] and thrombin (also known as blood clotting factor FII) [51–54]. Thrombin levels increased by 53 ± 11% in NHCY-CCI rat plasma at day 1-pi. This was potentiated by HHCY, resulting in 97 ± 35% increase (figure 6A, B; $p < 0.001$). These deficits in thrombin remained through day 7-post-injury.

Von Willebrand factor protein was barely detectable in the brain of NHCY-sham rats. HHCY increased vWF expression in sham's brain by 1.94 ± 0.75-fold at day 1-post-surgery and in NHCY-CCI rats, its expression was 5.45 ± 2.3-fold higher ($p < 0.05$). Noticeably, the combined effect of brain injury and HHCY further enhanced vWF immuno-reactivity, by 7.6 ± 3.8-fold than in NHCY-sham rats (figure 7A-B; $p < 0.01$). At day 7 post-surgery, vWF expression decreased in the brains of both NHCY- and HHCY-CCI rats compared to day 1 post-surgery however, vWF levels remained higher in HHCY-CCI rat relative to rats in other groups (figure 7B).

3.10 HHCY promotes inflammation and caused diffuse presence of inflammatory cells following TBI

Inflammation is an important hallmark of TBI pathophysiology and its occurrence can be demonstrated by the presence of cellular markers such the activated microglia or macrophages [29,30,55]. Macrophages are blood borne-inflammatory cells that invade injured brain regions [56,57]; with the mediation of cell adhesion molecules such as the intercellular adhesion molecule 1 (ICAM-1) [58–60]. CCI-induced brain injury caused an increase of ICAM-1 expressing cells, mostly confined to the penumbral around the lesion site in the motor/somatosensory 1-cortex among NHCY-rats at day 7 post-injury. These cells covered 4.3 ± 1.7-fold greater brain area than that of NHCY-sham rats ($p < 0.05$). By contrast, ICAM-1 positive cells in HHCY-CCI rats covered an area 9 ± 2.8-fold greater than that of NHCY-shams ($p < 0.001$) and 2.1 ± 0.87-fold than NHCY-CCI brain ($p < 0.05$). In these rat brains, ICAM-1 positive cells were also densely present in more distant cortical regions including the somato-sensory 2-cortex. To a lesser extent, ICAM-1 positive cells were also present in the brain of HHCY-sham rat brain where they were found mostly around blood vessels covering an area 1.9 ± 0.73-fold greater than that of NHCY-shams ($p > 0.05$).

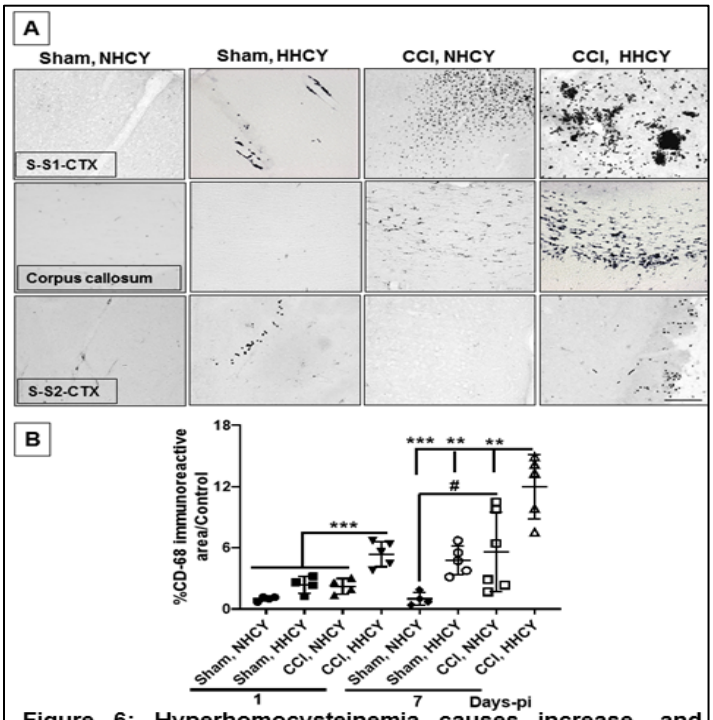

Figure 6: Hyperhomocysteinemia causes increase- and diffuse presence of inflammatory cells in the rat brain parenchyma. Representative microscopic images showing CD-68 immuno-positive cells in rats somatosensory 1 and 2 cortices and the corpus callosum at day 7 post-surgery. (B) Quantitation of the percent CD-68 immuno-positive brain area indicated that CCI injury caused a significant infiltration of inflammatory cells in the rat brain and that condition was exacerbated by HCY accumulation resulting in significantly greater area coverage by CD-68 positive cells (n = 5, *p < 0.05, **,##p < 0.01 and ***p < 0.001).

The presence and regional distribution of inflammatory cells demonstrated by CD-68 immuno-reactivity, a marker of activated microglia and microphages, correlated closely with that of ICAM-1. In NHCY-CCI rat brains, CD-68 positive cells showed a high density in the motor/somatosensory 1 cortex and low presence in regions such as the corpus callosum. At day1-pi, they covered in NHCY-CCI and

HHCY-CCI rat brains 2.2 ± 0.8-fold and 5.8 ± 1.2-fold respectively greater area compared to NHCY-shams (Figure 6; $p < 0.001$). At day 7-pi, CD-68 positive cells covered 5.59 ± 2.35-fold ($p < 0.05$) and 11.9-± 3.14-fold (Figure 6; $p < 0.001$) respectively in NHCY-CCI and HHCY-CCI rat brains versus NHCY-shams. Similar to ICAM-1, CD-68 positive cells were also present in HHCY-sham rat's brains, mostly around blood vessels covering of their brain.

3.11 Homocysteine accumulation enlarges CCI lesion volume

The observation of enhanced and broadening neuro-inflammation beyond the injury with HHCY suggested that penumbra tissue would be of elevated risk of death and widening of the CCI lesion. To assess this, we examined the impact of HHCY on TBI-induced lesion volume. CCI-induced brain injury caused a lesion volume of 2.81 ± 2.42mm^3 in NHCY-CCI rats compared to sham rats which exhibited only a mild craniotomy-induced scar averaging 0.23 ± 0.15mm^3 and 0.25 ± 0. 2mm^3 in NHCY-shams and HHCY-shams respectively. HHCY significantly exacerbated CCI-induced lesion volume to 5.45 ± 3.38mm^3 ($p < 0.05$, figure 7A, B). Taken together, these data show HHCY is inducting oxidative stress, BBB disruption, cortical neuro-inflammation, and that HHCY is worsening these neuropathological changes in mTBI along with significantly enlarging the cortical lesion volume.

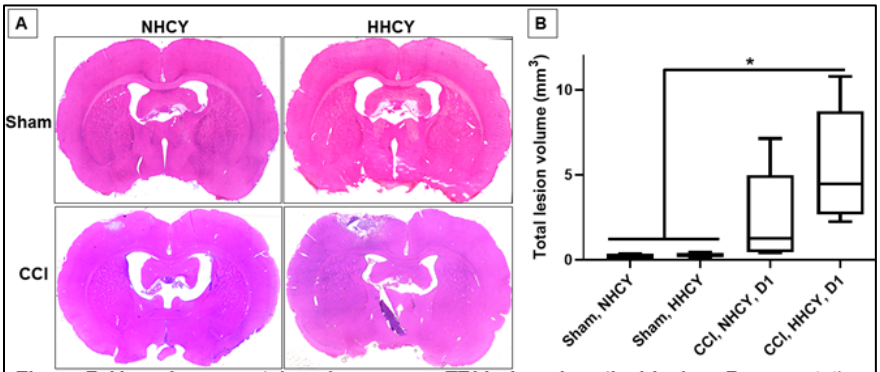

Figure 7. Hyperhomocysteinemia worsens TBI-induced cortical lesion. Representative hematoxylin and Eosin stained coronal brain sections showing cortical impact induced brain lesion. (B) Lesion volume quantitation showed that HHCY aggravated CCI-induced cortical brain lesion compared (n = 5; *p < 0.05), compared to sham rats.

3.12 Homocysteine worsens anxiety like behavior following CCI

HHCY's deleterious effects on multiple neuropathological findings in these animals suggests there may also be associated behavioral deficits. To investigate this, we used an Elevated Plus maze test to assess the effects HHCY on function performance. In this task animals travel between open and closed arms and is a classic test of anxiety like behaviors attributed to cortical and subcortical neural processing [61–63]. The total distance traveled during the test was not significantly different between groups, indicating HHCY impairment does to influence locomotor activity. There were also no significant differences in anxiety like behavior in NHCY-CCI rats

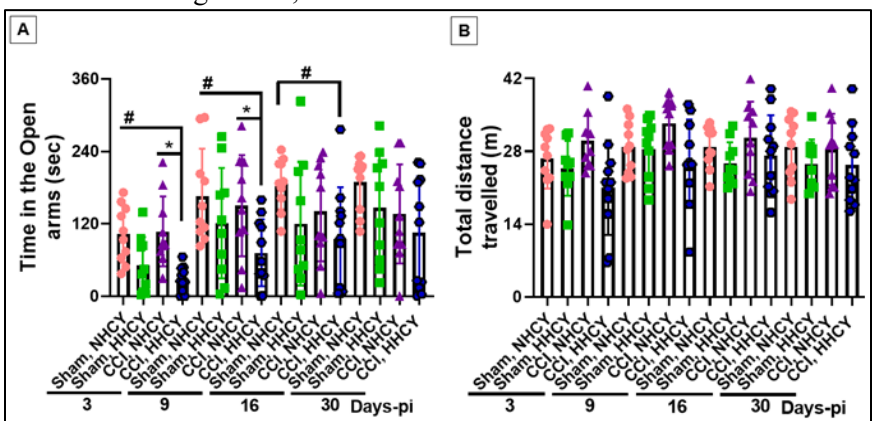

Figure 8. Homocysteine accumulation increases anxiety-like behavior in TBI rats. Graph illustrating the time spent by experimental rats in the open arms of the Elevated Plus maze. Hyperhomocysteinemia caused significant reduction of the time spent by CCI-rats exploring the open arms of the maze at days 3 and 9 post-surgery compared to NHCY-shams (n = 11; ##p < 0.01) and NHCY-CCI rats (n = 11; #p < 0.05). (B) The total distance travelled by rats in the maze was not different among rats in different experimental groups (n = 11; p > 0.05).

compared to both HHCY and NHCY-shams ($p > 0.05$; figure 11A). However, HHCY significantly increased anxiety in CCI rats on days 3 and 9-pi causing them to respectively spend just 28.4 ± 20.6s and 71.9 ± 55.6s in the Plus maze open arms compared to 107.3 ± 58.2s and 150.2 ± 83.9s for NHCY-CCI rats ($p < 0.05$; Figure 8A). Moreover, the detrimental effect of HHCY on anxiety like behavior remained significant in HHCY CCI-rats at day-16pi (95.3 ± 84.9s) compared to NHCY-shams that spent 186.9 ± 42.5s in the open arms of the maze; $p < 0.05$; Figure 8A). This suggests that the worsening of mTBI neuropathology when HHCY is present has a deleterious effect on anxiety like behaviors.

3.13 HHCY increased oxidative stress-induced nitrotyrosine in the dentate gyrus

We hypothesized that HHCY would elevate oxidative stress in the hippocampus. To determine the effect of HHCY on oxidative stress, we immuno-stained for the oxidative stress marker nitrotyrosine concomitantly with the neuronal marker NeuN to identify hippocampal architecture. Nitrotyrosine was expressed mainly in stellate shape cells across all layers of the dentate gyrus consistent with the morphology and distribution of astrocytes (Figure 9). Nitrotyrosine positive cells increased significantly in the dentate gyrus of HHCY-sham rats, 12,000 ± 5,237 cells/mm^3 compared to 1,100 ± 52 cells/mm^3 in NHCY-shams (Figure 9A, B; Q = 6.16, p <0.01), indicating HHCY in normal sham animals is a pro-oxidative stressor as predicted. HHCY also significantly potentiated the presence of nitrotyrosine positive cells in the DG of rats that sustained mTBI, 18,000 ± 5,863 cells/mm^3, compared to 7,200 ± 2,190 cells/mm^3 in NHCY-CCI rats (Figure 9A, B; Q = 5.75, p <0.01) to levels greater than in HHCY sham rats. This indicates that TBI and HHCY are close to additive on induction oxidative stress gene expression.

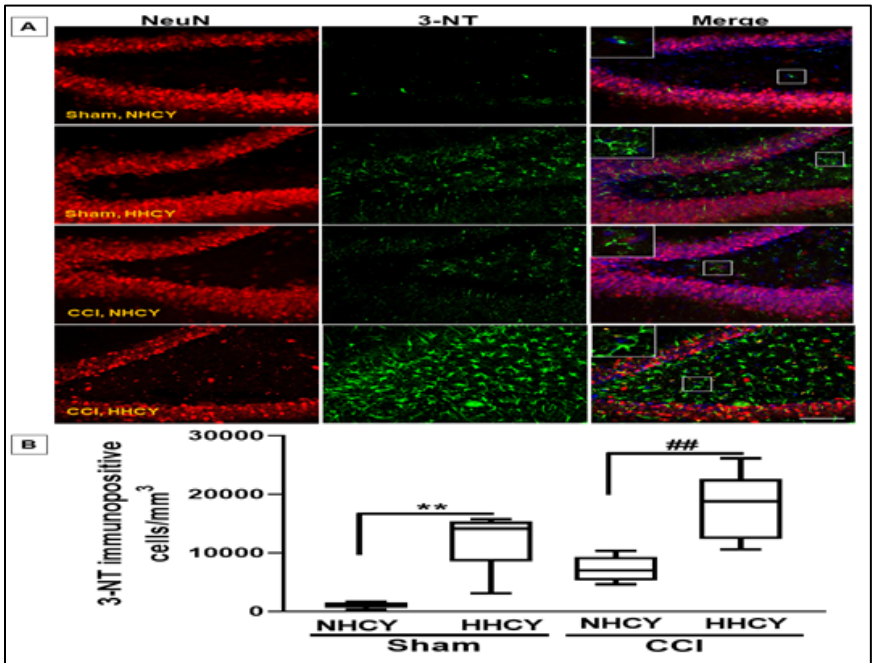

Figure 9. Increased nitrotyrosine expression in the dentate gyrus of brain-injured rats and exacerbation by HHCY. Representative of immune-fluorescent images demonstrating the presence of neuronal protein NeuN (red), oxidative stress marker nitrotyrosine (green), and DAPI used for nuclear counterstaining (blue) in the dentate gyrus of rat hippocampus. The scale bar is 100 µm. (B) Quantitation of nitrotyrosine positive cells showed that nitrotyrosine expressing cells were significantly higher in the dentate gyrus of HHCY sham and CCI rats 24hour post-injury compared NHCY-sham and -CCI rats, respectively (n = 5; **, ##$p < 0.01$).

3.14 Homocysteine accumulation suppressed tight junction protein expression and altered the ultrastructure of the vascular endothelial nucleus after mild TBI

Mild TBI and oxidative stress are both known to influence the blood brain barrier, which is formed by endothelial cells basement membrane, and astrocytic end-feet. To investigate the effect of HHCY on blood brain barrier, we assessed expression of the tight junction protein occludin following mTBI. Occludin expression decreased by 40.27 ± 4.2% in NHCY-CCI rat hippocampi on day 7 post-injury (pi) compared

to NHCY-sham rats (Figure 10A, B; $Q = 4.83$; $p < 0.05$). The presence of moderate HHCY aggravated the effect of mTBI on occludin expression, causing a 52.2 ± 2.9% and 48.1 ± 3.6% reduction respectively on days 1 and 7 pi compared to NHCY-shams (Figure 10A, B; $Q = 6.2$; $p < 0.01$). Moreover, there was a 32.5 ± 4.3% decrease in occludin express ion in the hippocampi of HHCY-CCI rats than NHCY-CCI rats on day 1 pi (Figure 10A, B; $Q = 5.12$; $p < 0.05$).

We next assessed if there were structural changes to the endothelium of the hippocampal microvasculature by determining if HHCY affected the ultrastructure of vascular endothelial cells following mTBI. Using a Transmission Electron Microscopy analysis of the hippocampal fissure region on day 1post-surgery (Figure 2C), we found that mTBI alone caused a significant increase of the length of the endothelial cell nucleus in NHCY-CCI rats, 3.42 ± 1.64 µm, compared to NHCY-sham rats, 1.88 ± 0.55 µm (Figure 10D, E; $Q = 3.7$; $p < 0.01$). The combination of mTBI and HHCY further increased the length of the endothelial cell nucleus in HHCY-CCI rats, 6.47 ± 1.82 µm, compared to NHCY-sham and NHCY-CCI rats ($Q = 10.9$ and 7.2 respectively; $p < 0.001$). Moreover, the endothelial cell nucleus width was also significantly increased in HHCY-CCI rats, 1.18 ± 0.55 µm compared to NHCY-CCI rats, 0.66 ± 0.23 µm, and NHCY-shams 0.51 ± 0.15 µm (Figure 10D, F; $Q = 4.78$ and 5.7 respectively; $p < 0.01$). Together, these data indicate significant molecular and structural changes associated with endothelial cell maintenance of the blood brain barrier integrity with mTBI that are exacerbated with HHCY.

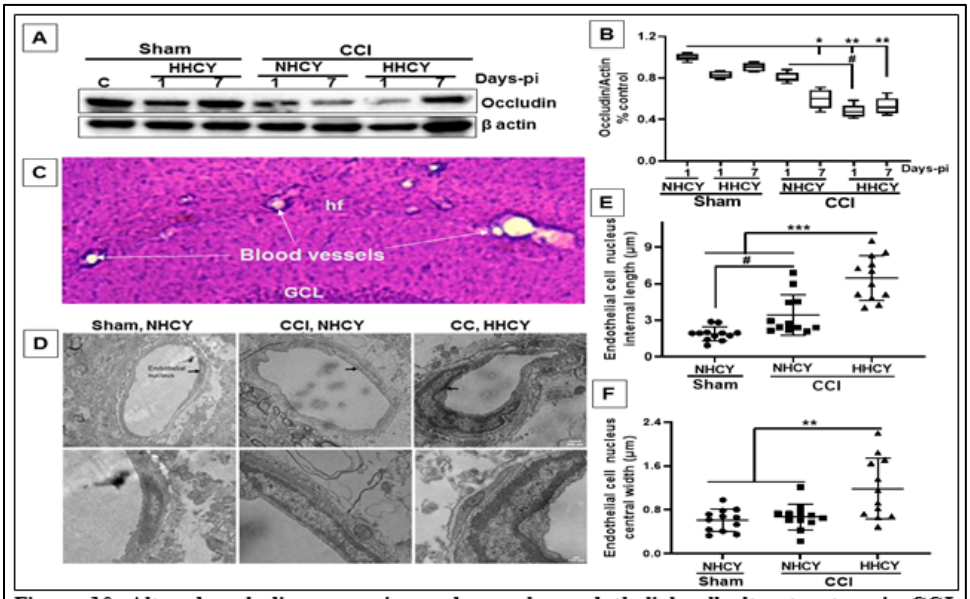

Figure 10. Altered occludin expression and vascular endothelial cell ultrastructure in CCI-injured rat brain hippocampus were worsened by HHCY. (A) Representative immunoblots illustrating the expression of occludin in rat hippocampus. (B) Quantitation of protein band intensities indicates that occludin expression was decreased in the NHCY-CCI rat hippocampus on day 7 post-injury. This reduction was more profound in the hippocampus of HHCY-CCI rats on days 1 and 7 post-injured (n = 5; *,#p < 0.05, **p < 0.01). Beta-actin was used as a loading control. (C) Representative image of hematoxylin and eosin staining of the hippocampal fissure (hf) region where microscope dissected brain sections were collected for the Transmission Electron Microscopy experiment. The image shows blood vessels and the granular cell layer (GCL). (D) Representative TEM images showing endothelial cells and their respective nucleus with a pointed arrow. The scale bar is 500 µm. (E-F) Quantitation of endothelial nucleus internal length and central width indicated a significant increase in endothelial cell nucleus internal length and central width in HHCY-CCI compared to HHCY-sham and NHCY-CCI rats (n = 11-12 cells/group; **p < 0.01, ***p < 0.001). There was also a significant increase in endothelial cell nucleus internal length in NHCY-CCI compared to HHCY-sham rats (n = 11-12 cells/group; #p < 0.05).

3.15 HHCY altered the hippocampal expression of apoptosis regulation proteins following mild TBI

3.15.1. HHCY increased the expression of cleaved caspase 3

Apoptotic cell death is a hallmark of multiple models of TBI and neural cellular stress. We examined the effects of HHCY on hippocampal apoptotic cell death following mTBI by staining for the presence of cleaved caspase 3 protein (CC-3). We found a significant increase in CC-3 immunoreactive cells in HHCY-sham rats, 2,660 ± 492 cells/mm^3 compared to NHCY-sham rats, 171 ± 75 cells/mm^3 (Figure 11A, B; Q = 5.4, $p < 0.01$). Greater differences were found between NHCY-CCI rat dentate gyrus, 3,977 ± 1,237 cells/mm^3 and NHCY-shams ($p < 0.001$). Moreover, the presence of CC-3 immunoreactive cells was significantly greater in the dentate gyrus of HHCY mTBI rats, 6,352 ± 1,563 cells/mm^3, compared to HHCY-shams and NHCY-CCI rats (Figure 11A, B).

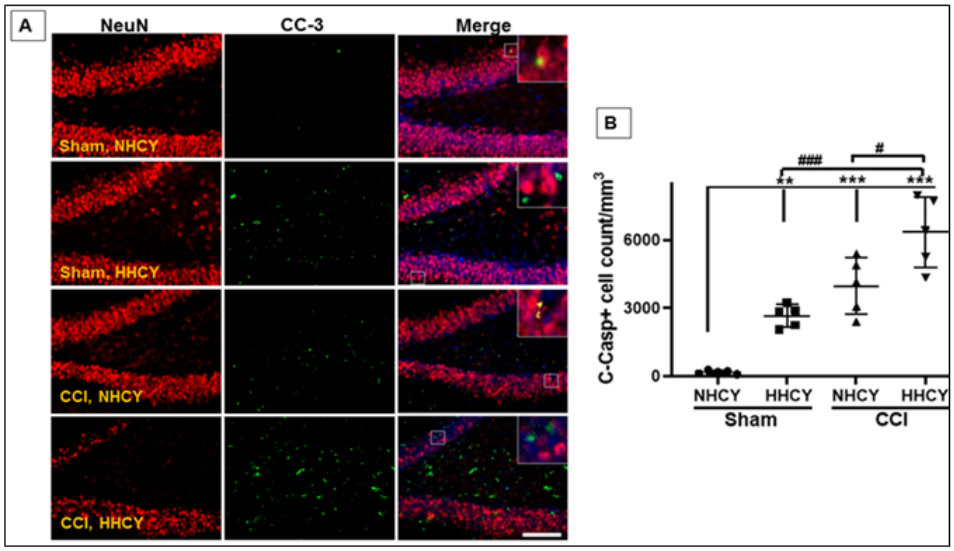

Figure 11: Brain injury-induced cleaved caspase 3 expression in the hippocampal dentate gyrus exacerbated by HHCY. (A) Representative immunofluorescent microscopic images showing cleaved caspase 3 (CC-3; green) and NeuN (red) immuno-positive cells, and DAPI stained nuclei in the dentate gyrus of HHCY and NHCY-CCI and sham rats on day 1 post-surgery. The scale bar is 100 µm. (B) Quantitation found a significant increase in CC-3 immunoreactive cells in the dentate gyrus of HHCY-sham and NHCY-CCI compared to NHCY-shams (n = 5; #p < 0.05, **p < 0.01 and ***, ###p < 0.001). This condition was aggravated in HHCY-CCI rat dentate gyrus, resulting in a significant increase of CC-3 positive cells in their dentate gyrus than those of HHCY-sham and NHCY-CCI rats (n = 5; #p < 0.05, ###p < 0.01).

3.15.2. Homocysteine accumulation upregulated BAX expression and α-ii spectrin proteolytic breakdown in the hippocampus of mild TBI rats

Following HHCY's impact on cleaved caspase 3 expressions in mTBI rats' dentate gyrus, we asked whether HHCY affected expression of the proteolytic breakdown pro-apoptotic proteins BAX and α-ii spectrin. We found a significant 1.44 and 1.57-fold increase in α-ii spectrin proteolytic breakdown products in HHCY-CCI rats' hippocampus on day 7 post-injury compared to NHCY-shams and HHCY-shams on day one post-surgery, respectively (Q = 4.16 and 4.99, $p < 0.05$, respectively). Similarly, BAX expression had a 1.66 and 1.69-fold increase in HHCY-CCI rats on days 1 and 7 post-injury, compared to HHCY-sham rats on day seven post-surgery (Q = 4.16 and 4.24 respectively, $p < 0.05$).

3.15.2. Homocysteine accumulation suppressed ERK and AKT phosphorylation following mild TBI

We next assessed the effect of HHCY on the phosphorylation of cell survival proteins ERK1/2 and AKT. We found that 1.8-fold reduced ERK phosphorylation in HHCY-shams and by 1.6-fold in NHCY-

CCI rats on day 7 post-surgery than NHCY-shams (Figure 12A, C; Q = 5.18 and 4.74 respectively, $p < 0.05$). Moreover, the combination of HHCY and mTBI further suppressed ERK phosphorylation by 2.15-folds on day 1 post-injury and by 2.5-folds on day 7 post-injury compared to NHCY-shams (Figure 12A, C; Q = 6.2 and 7.05 respectively, $p < 0.01$ and $p < 0.001$). On the other hand, mTBI alone had a biphasic impact on AKT phosphorylation at different experimental time points. On day 1 post-injury, pAKT levels increased significantly by 1.98-folds and 2.35-folds compared to HHCY-sham and HHCY-CCI rats (Figure 12B, D; Q = 5.43 and 6.61 respectively, $p < 0.05$ and 0.01). We also found a 2.1-folds significant decrease in pAKT levels in HHCY-CCI rats' hippocampi, compared to NHCY-shams (Figure 12B, D; Q = 5.7, $p < 0.05$).

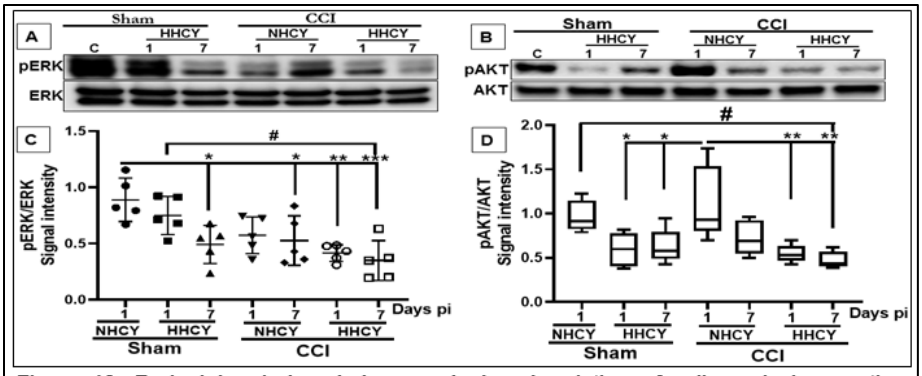

Figure 12: Brain injury-induced decreased phosphorylation of cell survival-promoting proteins ERK1/2 and AKT potentiated by HHCY Representative immunoblots illustrating the expression of phosphorylated and total ERK (A) and AKT (B) in hippocampal of NHCY or HHCY sham and CCI rats on days 1 and 7 post-surgery. Beta-actin is used as a loading control. (C, D) Quantitation of phosphorylated protein band intensities over the total protein showed a significant decrease in pERK in the hippocampus of NHCY-CCI and HHCY-sham rats on day 7 post-surgery compared to NHCY-shams (n = 5, *p < 0.05). HHCY aggravated pERK reduction on days 1 and 7 post-injury (n = 5; #p < 0.05, **p < 0.01 and ***p < 0.001). On the other hand, AKT phosphorylation was significantly increased in NHCY-CCI on day-1 post-injury compared to HHCY-sham and CCI rats (n =5; *p < 0.05, **p < 0.01). pAKT levels showed a significant reduction in the hippocampus of HHCY-CCI rats compared to NHCY-shams (n = 5; #p < 0.05).

3.15.3. Elevated homocysteine increased mild TBI-induced neuronal cell death

Given the enhanced expression of pro-apoptotic and suppressed expression of anti-apoptotic proteins observed above, we hypothesized that there would be significant cell death in the dentate gyrus. To determine apoptotic cell death changes in neuronal cell density in the dentate gyrus, we immuno-stained against the neuronal marker NeuN in the ipsilateral and contralateral dentate gyrus. mTBI alone significantly reduced neuronal cell density only in the ipsilateral DG of NHCY-CCI rats, 295877± 70341 cells/mm^3, compared to NHCY-shams and HHCY-shams (Figure 13A, B; Q = 10.62 and 4.3, $p < 0.01$ and 0.05 respectively). In contrast, we found a significant decrease of neuronal cell density in both the ipsilateral and contralateral dentate gyrus of HHCY-sham rats on day 1 post-surgery, 416,395 ± 55,464 cells/mm^3 and 433,932 ± 21,801 cells/mm3 respectively, compared to 592,889 ± 47,296 cells/mm^3 and 613,226 ± 30,645 cells/mm^3 for NHCY-shams (Figure 13A, B; Q = 6.31 and 10.77, $p < 0.01$ and 0.001). The combination of HHCY and mTBI substantially decreased neuronal cell density in the dentate gyrus ipsilateral and contralateral, 194,495 ± 22,242 cells/mm^3, and 290,445 ± 46,670 cells/mm^3 respectively, compared to other rats in other experimental groups (Figure 13A, B).This suggest that although the contralateral hippocampus in mTBI does not exhibit major loss of cells, the addition of HHCY is a potent neurotoxic insult, causing neural density loss in the contralateral hippocampus dentate gyrus was equivalent to the loss of cells on the ipsilateral injured side of the brain.

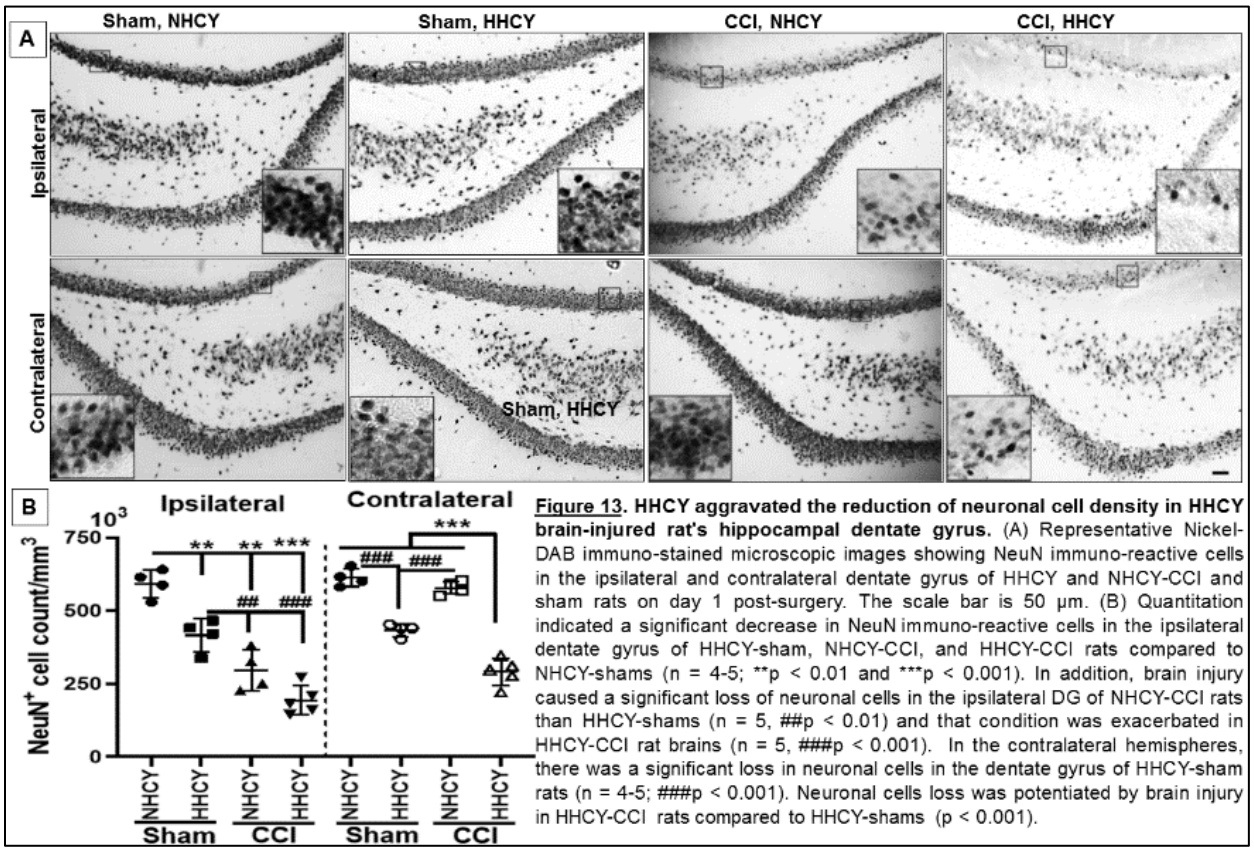

Figure 13. HHCY aggravated the reduction of neuronal cell density in HHCY brain-injured rat's hippocampal dentate gyrus. (A) Representative Nickel-DAB immuno-stained microscopic images showing NeuN immuno-reactive cells in the ipsilateral and contralateral dentate gyrus of HHCY and NHCY-CCI and sham rats on day 1 post-surgery. The scale bar is 50 µm. (B) Quantitation indicated a significant decrease in NeuN immuno-reactive cells in the ipsilateral dentate gyrus of HHCY-sham, NHCY-CCI, and HHCY-CCI rats compared to NHCY-shams (n = 4-5; **p < 0.01 and ***p < 0.001). In addition, brain injury caused a significant loss of neuronal cells in the ipsilateral DG of NHCY-CCI rats than HHCY-shams (n = 5, ##p < 0.01) and that condition was exacerbated in HHCY-CCI rat brains (n = 5, ###p < 0.001). In the contralateral hemispheres, there was a significant loss in neuronal cells in the dentate gyrus of HHCY-sham rats (n = 4-5; ###p < 0.001). Neuronal cells loss was potentiated by brain injury in HHCY-CCI rats compared to HHCY-shams (p < 0.001).

3.16. Homocysteine accumulation impaired hippocampus-dependent working memory performance in rats with mild TBI

The hippocampal formation is a key determinant in the process of working memory. We conjectured that the alterations in oxidative stress, blood brain barrier integrity, and neural cell loss present with our moderate HHCY and mild TBI could result in deficits in working memory. Using the Y maze test, a sensitive measure of short term working memory, we found that HHCY-CCI rats achieved significantly reduced spontaneous alternations on days 1 pi, 50.8 ± 13.5%, and on 7 pi, 46.76 ± 19.36% compared respectively to 72.9 ± 9.58% and 73.89 ± 11.44% for HHCY-shams (Figure 14D; Q = 5.16, 6.34 respectively, $p < 0.05$ and 0.01). Mild TBI alone had no significant impact on working memory performance. However, HHCY alone caused a delayed but significant deficit on the working memory performance of shams rats on day 14 post-injury, 53.54 ± 10.52% compared to 71.1 ± 18.8% for NHCY-sham rats (Figure 14D, Q = 4.03, $p < 0.05$). Moreover, HHCY also prolonged the time some mTBI rats took to complete their first spontaneous alternation in the Y maze device. Consequently, some of these animals completed a spontaneous alternation after 77 secs in the Y maze. Simultaneously, NHCY-sham and NHCY-CCI had completed 3 or more spontaneous alternations (Figure 14A-C)

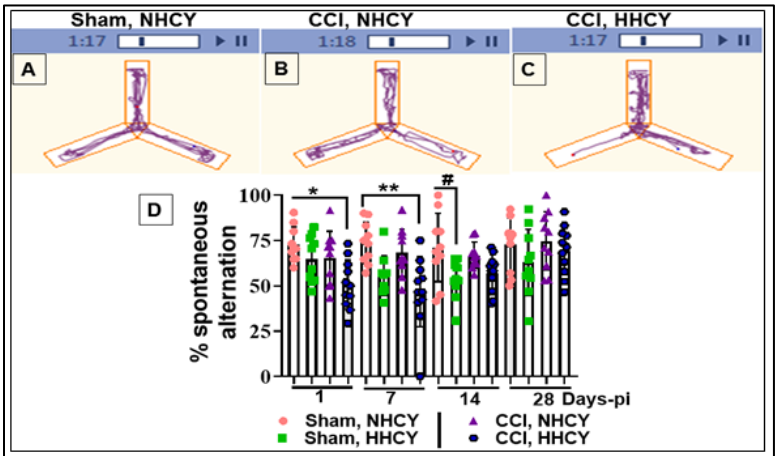

Figure 14: HHCY caused a significant reduction of the percent spontaneous alternation of experimental rats in the Y maze: (A-C) Images of the Y maze exploration tracks showing the exploration frequency of NHCY and HHCY-sham and CCI rats in the Y maze device during the working memory performance test. This shows that HHCY-CCI mice completed their first alternation after up to 77 secs in the maze, while rats in other groups had achieved 3 or more spontaneous alternations at that time. (D) Graph of the Y maze test results demonstrating that HHCY-CCI rats had significantly reduced % spontaneous alternation in the Y maze on days 1 and 7 post-injury compared to NHCY-shams (n = 10-12; *p < 0.05, **p < 0.01). Delayed detrimental effects of HHCY on sham rats was observed, resulting in significantly reduced % spontaneous alternation on day 7 and 14 post-surgery compared to NHCY-shams (n = 10-12; #p < 0.05, **p < 0.01).

3.17 Chronic psychological stress significantly increased plasma homocysteine levels

Using a clinical-grade enzymatic assay (Diazyme labs., CA), we measured plasma HCY levels in Rst and NRst CCI and sham rats on days 1 and 7 pi. Results found on day 1 pi, 1.8 and 2-folds increases in HCY levels in Rst-sham (10.44 ± 2.47 µM) and Rst-CCI (12.82 ± 4.65µM) compared respectively to NRst-sham (5.44 ± 2.23µM) and NRst-CCI (5.95 ± 1.37µM); n = 8, $p < 0.01$. Similar changes were observed on day 7 pi. 50-60% of the restraint rats presented HHCY clinically defined as plasma HCY concentration ≥ 15 µM defined in humans[36,37].

3.18 Mild traumatic brain injury-induced oxidative stress was exacerbated by chronic psychological stress

We measured two oxidative stress markers, plasma malondialdehyde levels and levels of 4-hydroxynonenal in three brain regions, including the hippocampus and prefrontal cortex, which are brain regions that are very vulnerable to oxidative stress, and in the parietal cortex, which close to the impact site. Plasma malondialdehyde levels measured using a TBARs Assay kit (Cayman Chemical, MI) showed significant increases of malondialdehyde in Rst-CCI rats on day 7 post-injury, 1.38 ± 0.25µm, compared to 1.07 ± 0.08µm and 1.01 ± 0.12µm in NRst-CCI and NRst-sham rats (n=6 rats/group; $p < 0.05$).

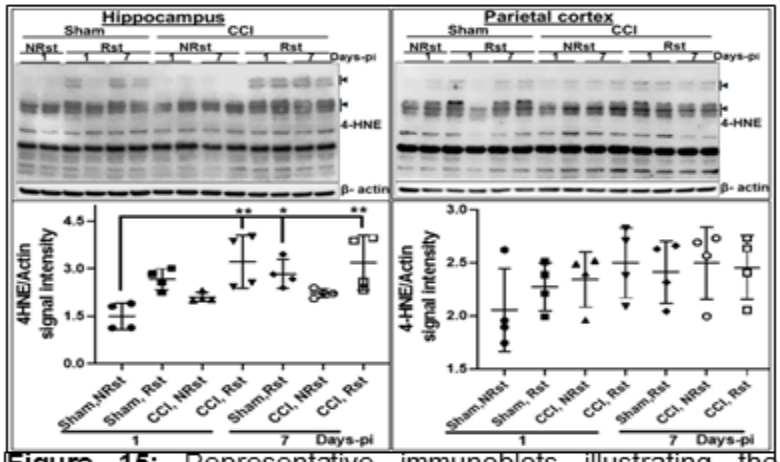

Figure 15: Representative immunoblots illustrating the expression of 4-hydroxynonal in the HP and PT on days 1 and 7 post-injury. Graphss show quantitation of 4-HNE signal intensity in the HP and PT using actin as loading control. (n = 4; *p < 0.05 and **p < 0.01).

Western blot analysis found significant increases in 4-hydroxynonenal (4-HNE) in the PFC and HP of Rst-CCI and Rst-sham rats compared to NRst-sham and NRst-CCI rats. Remarkably, Rst rats showed specific bands at 100-105 kilodalton (kdal; (Figure 15, arrow 1) in the PFC and HP that did not exist in NRst rats. In addition, bands at 70-55 kdal were broader in Rst than in NRst in these brain regions (Figure 15; arrow 2). By contrast, the 100-105 kilodalton (kdal) bands were present in the parietal cortex of Rst rats as well as the NRst-CCI rats (Figure 15).

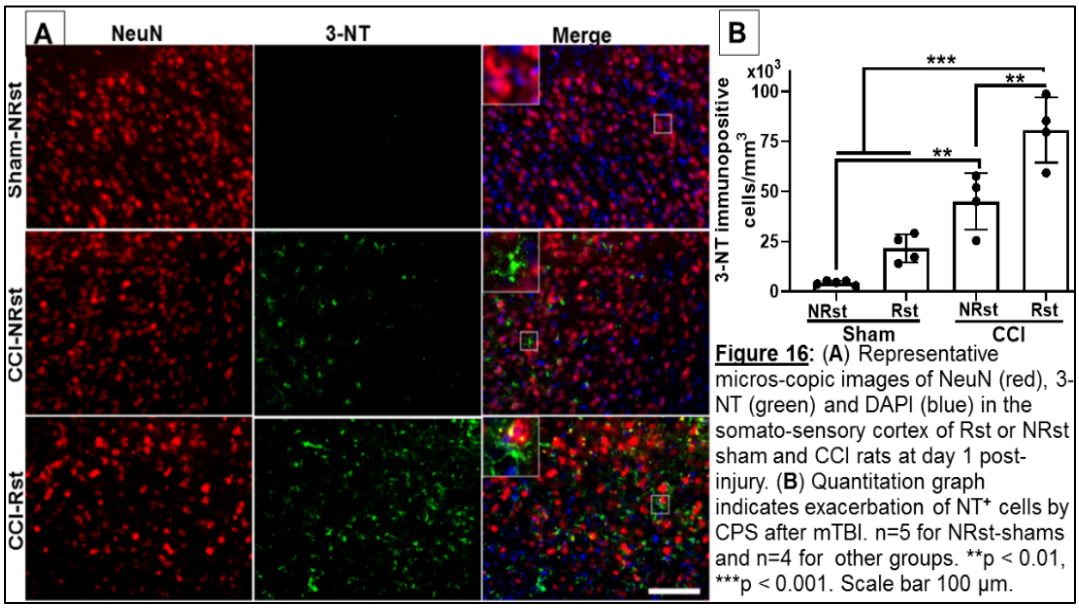

Figure 16: (**A**) Representative micros-copic images of NeuN (red), 3-NT (green) and DAPI (blue) in the somato-sensory cortex of Rst or NRst sham and CCI rats at day 1 post-injury. (**B**) Quantitation graph indicates exacerbation of NT+ cells by CPS after mTBI. n=5 for NRst-shams and n=4 for other groups. **p < 0.01, ***p < 0.001. Scale bar 100 µm.

We also assessed the impact of CPS on oxidative stress following mTBI using fluorescent co-histoimmunostaining against nitrotyrosine (3-NT, a marker of oxidative stress), and NeuN (a marker of neuronal cells). Results showed that 3-NT expression in neuronal cells was limited to brain tissues at the impact site of Rst and non-restraint (NRst) TBI rats. Remarkably, 3-NT was also predominantly expressed in astrocyte-like cells with multiple processes (Figure 16A, the small panel in the "Merged" is magnified

4X) in the somatomotor cortex adjacent to the impact site of TBI animals and often in the somatosensory cortex beyond the impact site. We counted 3-NT positive (3-NT$^+$) cells in the somatomotor and somatosensory cortex regions using the unbiased optical fractionator method of Stereology (MBF, VT). We found a significant 2- and 4.2-folds increase in 3-NT$^+$ cells in the cortices of Rst and NRst sham rats respectively, compared to NRst-TBI rats. These differences further increased to 3.8 and 12-folds compared to Rst-TBI rats. Furthermore, we noticed a significant 1.8-fold increase in 3-NT$^+$ cells in Rst-TBI rats than NRst-TBI rats (Figure 16B)

3.20 Restraint-induced chronic psychological stress worsened mild TBI associated decrease expression of tight junction proteins occludin and zona occludens

We used western blot analysis to assess the effects of CPS on mTBI associated decreased expression of the tight junction proteins occludin and zona occludens 1 (ZO-1). Results found that restraint-induced CPS alone decreased ZO-1 expression in PFC, which was aggravated in RST-CCI rats where a substantial decrease in ZO-1 expression was observed on days 1 and 7 pi (Figure 17A, B). A similar ZO-1 expression pattern was observed in the HP. By contrast, in the PTC, the combination of restraint and mTBI caused a significant decrease in ZO-1 expression on day 7-pi compared to NRst-shams. Moreover, occludin expression was significantly suppressed in the PFC of Rst-CCI rats at days 1 and 7 pi compared to sham rats (Figure 17A, B). No significant change was found in the PTC.

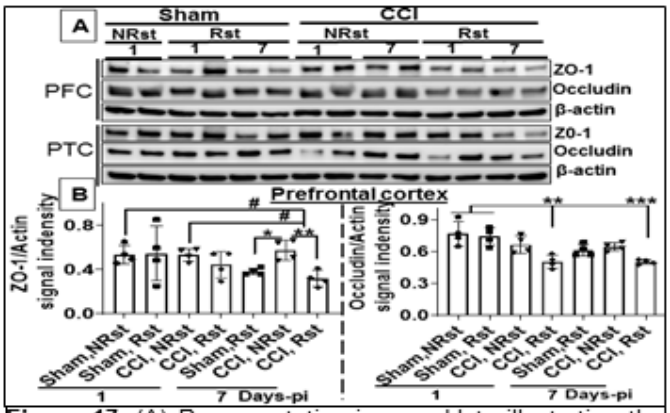

Figure 17: (A) Representative immunoblots illustrating the expression of tight junction proteins ZO-1 and occludin in the PFC and PTC on days 1 and 7 post-surgery. (B) Quantitation of signal intensity of occludin and ZO-1 bands in the PFC using actin as loading control. (n = 4; *p < 0.05, **p < 0.01). ***p < 0.001

3.21 Chronic psychological stress caused systemic and cerebral inflammation mediated by 4-hydroxynonenal adduct of the non-receptor tyrosine kinase protein

4-HNE is a lipid peroxidation end product, which under pathological conditions adducts to macromolecules and serves as a second messenger of free radicals by acting as signaling or cytotoxic molecules[64–66]. Interestingly, 4-HNE was shown to adduct and activate macromolecules such as the non-receptor tyrosine kinase (SRC)[67], which subsequently stimulates the formation of pro-inflammatory molecules such as NF-kB and COX-2. We immunoprecipitated 4-HNE from brain supernatant samples derived from the PFC and HP of Rst and NRst shams and CCI rats to explore that possibility. Immunoblotting analysis of immunoprecipitation isolates with an antibody against phosphorylated SRC revealed 60 kdal

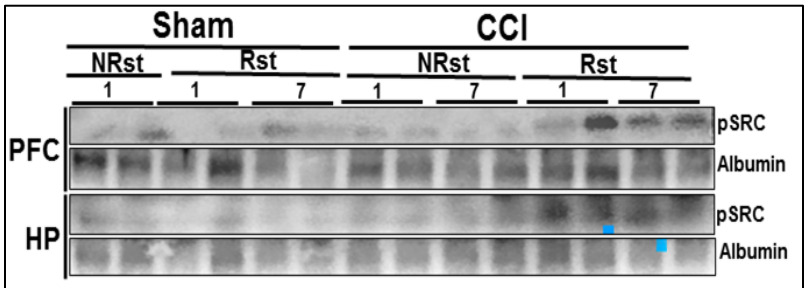

Fig. 18: Immunoblots images of showing pSRC immuno-reactive bands from 4-HNE immunoprecipitation isolates derived from restraint and non-restraint-shams and CCI rats PFC and HP brain homogenates. Albumin was used as 4HNE adduct control. (n = 2, loaded side by side)

bands in the PFC and HP of Rst-CCI rats on days 1 and 7-pi. Albumin was used as a positive control for 4-HNE adduction (Figure 18).

Under pathological conditions, increased 4-HNE activates proinflammatory molecules such as NFk-B and COX-2[66,68]. Using western blot analysis, we measured Nuclear Factor kappa B (NFkB) expression in the PFC and HP. Results showed a significant 1.6-fold increase in NFk-B expression in the PFC on days 1 and 7-pi in Rst-sham rats compared to NRst-sham. In the PFC Rst-CCI rats, the difference in NFk-B levels was 1.4-folds higher on day 1-pi compared to Nrst-CCI rats (Figure 19A, B). More significant differences of 2.9 and 2.7-folds increase were found in the HP of Rst-sham rats on days 1 and 7 pi, respectively, compared to NRst-shams. In Rst-CCI, a 2.8-fold increase in NFk-B levels was found on day 7-pi compared to NRst-CCI rats (Figure 19C, D).

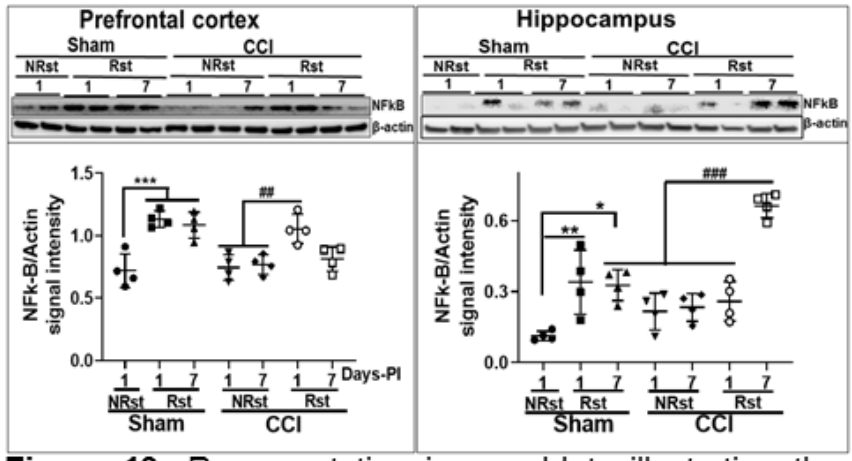

Figure 19: Representative immunoblots illustrating the expression of NFk-B in the PFC and HP of Rst and NRst-CCI and sham rats on days 1 or 7 post-injury. Graphs show quantitation of NFk-B bands signal intensity using beta actin as loading control. n = 4; *p < 0.05; **,##p < 0.01 and ***,###p < 0.001

Histo-immunostaining for CD68 protein (a marker of activated microglia/macrophages) was used to measure the density of inflammatory cells in the somatomotor and somatosensory cortex regions of Rst and NRst CCI and sham rats. Results found that chronic psychological stress-induced 4-HNE adduction of the non-receptor tyrosine kinase and upregulation NFk-B expression resulted in a significant 1.92-fold increase of CD68 positive cells in Rst-CCI rats compared to NRst-CCI. Similarly, we observed a 2.1-fold increase in CD68 positive cells in the same brain regions of Rst-sham compared to NRst-sham rats (Figure 20A-B). The CD68 positive cells density was significantly less in Rst-sham than Rst-CCI-rat brains. In Rst-sham rats, CD68 immunoreactive cells were primarily present around blood vessels, which may be due to the impact of restraint-induced CPS on BBB disruption (Figure 20A).

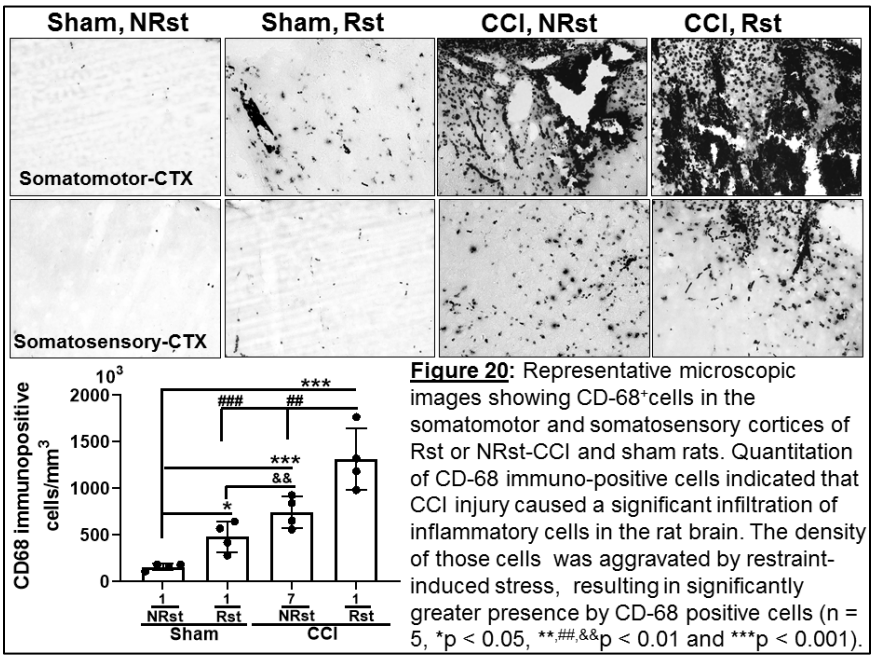

Figure 20: Representative microscopic images showing CD-68+cells in the somatomotor and somatosensory cortices of Rst or NRst-CCI and sham rats. Quantitation of CD-68 immuno-positive cells indicated that CCI injury caused a significant infiltration of inflammatory cells in the rat brain. The density of those cells was aggravated by restraint-induced stress, resulting in significantly greater presence by CD-68 positive cells (n = 5, *p < 0.05, **,##,&&p < 0.01 and ***p < 0.001).

We also measured using an ELISA kit (Sigma, MO), the plasma levels of c-reactive protein (marker of systemic inflammation) in Rst and

NRst- sham and CCI rats. Our results showed significantly elevated C-reactive protein levels in Rst-sham rats (13.03 ± 1.98 ηg/mL) compared to NRst-sham rats (9.5 ± 1.04 ηg/mL; $p < 0.05$). C-reactive protein levels were aggravated in Rst-CCI rats (14.17 ± 1.63ηg/mL) compared to NRst-CCI rats (10.05 ± 2.45 ηg/mL; $p < 0.01$). These differences were sustained on day 7 pi in Rst-sham rats (12.09 ± 2.86 ηg/mL) compared to NRst-sham rats (9.2 ± 1.37ηg/mL; $p < 0.05$). In Rst-CCI rats, C-reactive protein levels were 13.82 ± 4.16 ηg/mL compared 9.87 ± 2.95 ηg/mL for NRst CCI rats ($n = 4$; $p < 0.05$). These data suggest CPS promotes systemic inflammation in our model.

3.22 Impact of chronic psychological stress-induced oxidative stress and inflammation on brain cell death in rats with mild TBI

Oxidative stress and inflammation are usually associated with brain cell death. Brain sections were immunostained against cleaved caspase 3 (C. casp-3), a marker of apoptotic cell death and NeuN, to explore the potential effect of these CPS-induced pathological changes on neuronal cell death in rats with mTBI. C. casp-3$^+$ cells were counted in the somatomotor and somatosensory cortical regions, consistently with the inflammatory cells and 3-NT$^+$ cell counts described earlier. We observed a significant 3.2- and 5-folds increase in C. casp-3 $^+$ cell count in Rst and NRst sham rats respectively, compared to NRst- TBI rats. These differences were respectively increased to 13.6 and 25-folds compared to Rst-TBI rats. Moreover, we also found a significant 2.1-fold increase in C. casp-3$^+$ cells in Rst-TBI rats compared to NRst-TBI rats (Figure 21A, B). the small panel in the "Merged" is magnified 4X). Using high objective magnification (x63), we examined 250 cells from three serial sections from two Rst-TBI rats and determined that 85% of the C. Casp-3$^+$ cells co-expressed NeuN. We also co-immunostained these sections with antibodies against C. casp-3 and glial fibrillary protein (GFAP), a marker of astrocytes and found that C. casp-3$^+$ cells did not overlap with GFAP$^+$ cells (data not shown). This observation suggests that other brain cell types such as oligodendrocytes, which apoptotic death is known to contribute to TBI-associated demyelination, may account for non-neuronal C. casp-3$^+$ cells.

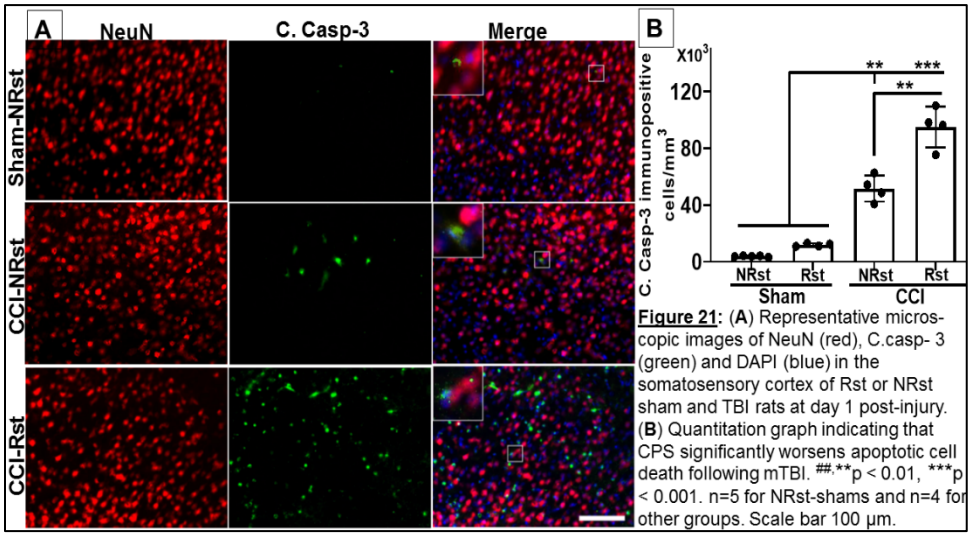

Figure 21: (**A**) Representative micros-copic images of NeuN (red), C.casp- 3 (green) and DAPI (blue) in the somatosensory cortex of Rst or NRst sham and TBI rats at day 1 post-injury. (**B**) Quantitation graph indicating that CPS significantly worsens apoptotic cell death following mTBI. ##,**$p < 0.01$, ***$p < 0.001$. n=5 for NRst-shams and n=4 for other groups. Scale bar 100 µm.

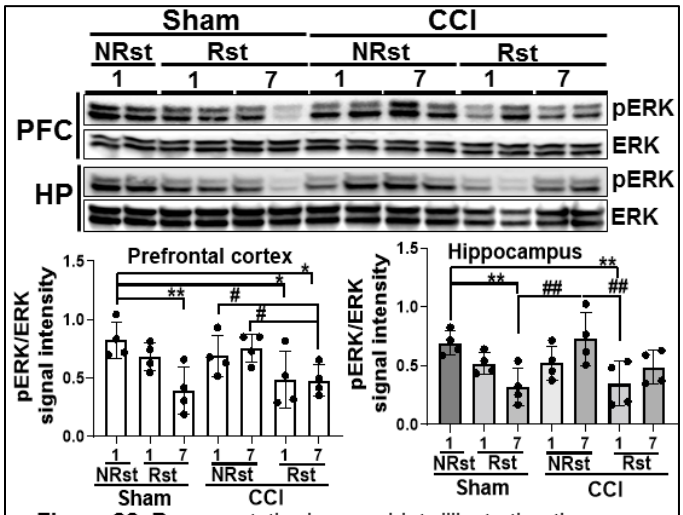

Figure 22: Representative immunoblots illlustrating the expression of ERK, pERK in the PFC and HP of Rst and NRst-sham and CCI rats on days 1 and 7 post-injury. Graphs show quantitation pERK bands signal intensity, using ERK as loading control. n = 4; *, #$p < 0.05$, **$p < 0.01$

We also used western blot analysis to measured phosphorylated and total levels of the extracellular signal-regulated kinase (ERK)1/2 in the PFC and HP. Results showed a 2-folds decrease in pERK expression in the PFC of Rst-sham rats than NRst-shams on day 7-pi. In addition, a 1.7-fold reduction in pERK expression was observed in Rst-CCI rats on days 1 and 7-pi compared to NRst-CCI rats (Figure 22A, B). In the HP, we found a 2.5-fold decrease in pERK expression in Rst-sham rats compared to NRst-shams. A similar difference was found between Rst-CCI and NRst-CCI (Figure 22A, C). These results suggest that CPS suppresses the anti-apoptotic signaling ability of brain cells in vulnerable stress regions, which worsens the pathology in rats.

3.23 Chronic psychological stress exacerbated mild traumatic brain injury associated impairments in anxiety-like behaviors, fine motor activity and delayed effects on hippocampal dependent working memory

Behavioral assessments conducted on our restraint-induced psychological stress model showed significantly increased anxiety-like behavior and increased deficits in fine motor coordination among Rst-CCI rats that persisted up to two weeks post-injury compared to NRst-shams or NRst-CCI rats. In summary, a significant increase in anxiety-like behavior was observed among Rst-CCI and NRst-CCI rats on day 2-pi compared to NRst-shams. This deficit was more profound in Rst-CCI rats (Figure 23A). After that, NRst-CCI rats recovered while the deficit persisted in Rst-CCI rats, resulting in a significant difference on days 8 and 15-pi compared to NRst-CCI rats (Figure 23A). Similar differences were observed with fine motor coordination (Figure 23B). Notably, the effects of restraint-induced CPS on working memory were delayed and the first significant effects was observed on day 15 pi when NRst-sham had 70.35 ± 7.48% alternation and Rst-CCI rats 57.59 ± 5.69% ($p < 0.05$). Furthermore, Rst-CCI rats exhibited more deficits in working memory while NRst-CCI rats showed sustained recovery at day 15 pi. Rst-CCI rats had 52.3 ± 6.09% alternation compared to 76.6 ± 7.63% and 71.23 ± 6.35% for NRst sham and NRst-CCI rats respectively ($p < 0.001$). Rst sham rats also had significantly poor Y maze performance at this time point, 63.99 ± 8.95%, compared to NRst shams ($p < 0.05$).

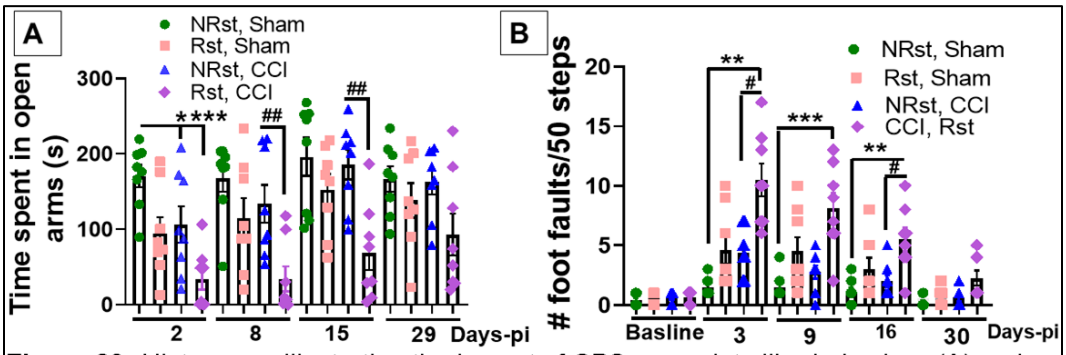

Figure 23: Histograms illustrating the impact of CPS on anxiety-like behaviors (A) and fine motor coordination (B). N = 10-12/group; *, # p < 0.05; **, ##p < 0.01 and ***p < 0.001.

3.24 Effects of Omaveloxolone treatments on glutathione and homocysteine metabolism

The therapeutic potential of Omaveloxolone (RTA-408) was preliminary assessed in our model of HCY-induced physiological stress. The compound was administered to normohomocysteinemia and hyperhomocysteinemic rats that sustained mTBI by controlled cortical impact. RTA-408 (20mg/kg), was done once daily for seven days-pi, significantly increased plasma glutathione levels in normo-HCY-CCI rats, 29.82 ± 6.59 µM, compared to vehicle-treated normo-HCY-CCI rats, 0.87 ± 0.34 µM, and HHCY-CCI rats 0.63 ± 0.37 µM (n = 4/group; $p < 0.001$). In addition, GSH levels were significantly higher in RTA-408 treated normo-HCY-CCI rats than in RTA-408 treated HHCY-CCI rats, 5.43 ± 0.56 µM (n =

4/group; $p < 0.01$). This result suggests a continuous use of GSH to mitigate HHCY-induced oxidative stress in these rats, compared to RTA-408 treated normo-HCY-CCI rats that suffer less oxidative stress burden. Importantly, RTA-408 treatment reduced plasma HCY levels by 18% among normo-HCY-CCI rats and 25% among HHCY-CCI rats, therefore supporting our belief that RTA-408 treatment facilitates HCY metabolism through the transsulfuration pathway to promote increased GSH formation. The 20mg/kg RTA-408 dose selection was based on the report by Shekh-Ahmad and colleagues that showed a broad spectrum therapeutic action of this dose in their mouse seizure model[69]

4.0 DISCUSSION:

4.1 Hypobaria exposure, oxidative stress and homocysteine transsulfuration association to glutathione oxidation in rats with mild TBI

Reports from several investigators suggest that flying at high altitude is associated with increased physiological stress [77,78], thus representing a risk for TBI patients who require aeromedical evacuation for advanced care. Results from the present study indicate that exposure of rats with mTBI, which represents up to 80% of all TBI cases [79,80], to hypobaria induces an acute increase of neural oxidative stress, which subsequently triggers an enhanced response of the antioxidant defense system that uses HCY and glutathione in a compensatory attempt to attenuate free radical formation.

Levels of oxidative stress markers malondialdehyde and superoxide increased in rats subjected to mTBI 2h post-hypobaria. This observation suggested that oxidative damage during aeromedical evacuation produced changes that could represent targets for therapeutic interventions. This is a crucialconcept, as unmitigated free radical formation mediates the induction of many TBI pathological markers,including inflammation and neuronal degeneration exacerbated by hypobaria exposure [2–4,81–83]. Therefore, our findings suggest that hypobaria-induced oxidative stress is a significant mediator or indicator of TBI pathological progression during and after hypobaria exposure.

Hypobaria-induced oxidative stress was coupled with very low to undetectable plasma HCY (Figure 1). HCY is a non-proteinogenic amino acid with substantial cytotoxic potential when accumulated[50,84,85]. Therefore, its metabolism is tightly regulated to ensure it is continuously eliminated [86,87]. This occurs via its remethylation to methionine, its precursor, or its transsulfuration to cystathionine, contributing to the downstream formation of glutathione, a very potent antioxidant [86,88]. Therefore, we postulated that the drastic reduction of HCY levels under oxidative stress at two-hour post-hypobaria wasindicative of its flush through the transsulfuration pathway. This hypothesis was potentiated by a significant increase of glutathione oxidation resulting in a two-fold increase of oxidized glutathione versusreduced glutathione at two hours post-hypobaria exposure (Figure 2A, B). The return of oxidized glutathione to baseline levels at day 30 post-exposure suggests an attenuation of oxidative stress. This observation correlates with significantly improved anxiety-like behavior to that of normobaric-sham rats.The therapeutic potential of HCY transsulfuration to promote glutathione formation has been underscored in several neurological disorders. For instance, the supplementation of N-acetylcysteine to promote glutathione biosynthesis through the transsulfuration pathway was neuroprotective in models of Huntington's disease [89,90], Alzheimer's disease [91,92], and TBI [93,94]. Moreover, this therapeutic approach isin a trial for pediatric TBI management [95].

Glutathione has free radical scavenging and anti-inflammatory properties [96,97]. Its metabolism is regulated by genes, including *GS,* which controls its biosynthesis through the transsulfuration pathway, and *GPx*, which catalyzes glutathione oxidation to attenuate free radical formation [86,88]. GPx has eight isozymes, among which isozymes 1 and 4 are abundant in the brain [98–101]. We analyzed the transcriptional profile of

these genes in the prefrontal cortex and the hippocampus that are very vulnerable to oxidative stress [102–105] and the parietal cortex around the cortical injury penumbra region. The upregulation of GS and GPx in the prefrontal cortex attests to its vulnerability to oxidative stress relative to its distant location to the injury region in the parietal cortex. In the parietal cortical, the combination of CCI and hypobaria resulted in an increase in GS and GPx that was not present with CCIor hypobaria alone. This suggests that the CCI penumbra region may be uniquely stressed by a synergy between the injury and hypobaria. To our knowledge, this study is the first to describe changes in glutathione and associated gene expression in a model of TBI and Hypobaria exposure.

Although the mechanism for the distinctive expression patterns in different brain regions is not fully elucidated, increased GPx expression in the cerebral cortex of aged rats was associated with higher astrocyte density [106]. Furthermore, GPx activity was derived primarily from astrocytes relative to neuronsin chicks' forebrain [107]. Also, increased GPx expression or glutathione oxidation was reported in severaloxidative stress associated with neurological disorders [108,109].

In summary, this study provides evidence that hypobaria exacerbates oxidative stress in rats with mTBI. This was associated with an enhanced flush of HCY through the transsulfuration pathway to promote glutathione biosynthesis, which is necessary to attenuate free radical formation. Increased glutathione metabolism was putatively driven by the upregulation of glutathione metabolizing genes, suggesting that enhanced glutathione metabolism represents a therapeutic target for TBI management.Further studies would be needed to understand how this antioxidant redox system would respond to interventions during and after hypobaria exposure following moderate to severe TBI.

4.2 Hyperhomocysteinemia and the pathophysiology of mild TBI-induced cortical injury

Genetic, epigenetic, and physiologic factors all influence TBI pathological outcome and contributeto the heterogeneity observed in the recovery trajectory of patients. This complexity hinders efforts to develop effective therapeutic agents for TBI management, and it is likely there will need to be multiple treatment options developed based on a patient individual status [110]. This study presents novel findings on the detrimental effects of HHCY on TBI-associated oxidative stress, blood-brain barrier alterations, inflammation, lesion size, and functional deficit in adult rats.

Oxidative stress is an essential hallmark of the TBI secondary injury process that causes the production of reactive species and mediates several TBI-associated pathophysiological events, including BBB damage[111,112], neuroinflammation [82,113], and cell death. Our results showed that HCY accumulation aggravated TBI-induced oxidative stress in the cortex with increased lipid peroxidation and nitric oxide, as demonstrated by increased levels of oxidative stress markers 4-HNE and 3-nitrotyrosine in the brain of HHCY-CCI-rats. Other studies have reported that HHCY triggers increased nitrotyrosine expression by suppressing the expression of dimethylarginine-dimethylaminohydrolase and causing the accumulation of asymmetric dimethylarginine (ADMA), an inhibitor of nitric oxide synthase. This subsequently caused increased nitrotyrosine formation from peroxynitrite[114,115]. 4-HNE, the major aldehyde produced during lipid peroxidation of polyunsaturated fatty acid, is upregulated after brain injury[116,117]. In our study, 4-HNE expression was significantly increased in the cortex of both HHCY-sham and -CCI rats. Consistent with our observation Lee and colleagues previously reported that increase 4-HNE following ischemic brain injury correlated with increased HCY levels [118].

Damage to the blood-brain barrier also plays a crucial role on the brain pathophysiology and disease progression [119]. This is influenced by changes in different components of BBB integrity, includingtight junction proteins and intercellular adhesion molecules[32,38,39,120]. Our assessment of the effects of HHCY on TBI-associated BBB dysfunction demonstrated its detrimental impact on the expression levelsof two

significant tights junction proteins, occludin and Zona occludens (ZO-1). While HHCY decreased the expression of occludin in cortical tissues of sham rats and CCI rats equally, the combination of injuryand HHCY exacerbated the suppressed expression of ZO-1 in addition to the occludin changes. These biochemical changes were paralleled by increased Evans blue extravasation, a test for BBB integrity, which persisted through day 7 post-surgery, substantiating the detrimental effect of HHCY BBB dysfunction following mTBI. Our observations are strengthened by a recent report by Kamat and colleagues [120] demonstrating the decreased expression of tight junction protein claudin 5 in the brain of intracerebrally injected-HCY mice and another study showing increased Evans blue extravasation in cystathionine beta-synthase deficient-hyperhomocysteinemic mice[19]. The effect of HHCY on BBB permeability may be related to HCYability to cause vascular microbleeding, which intensity is known to affect disease prognosis [121,122].

Subdural hemorrhage following mTBI modeled in this study impairs brain homeostasis and triggers several pathologic and compensatory responses associated with blood clotting and hemoglobinderived-iron storage[59–61,123]. Our results in NHCY-CCI rats concur with previous findings demonstrating increased vWF factor protein expression after TBI[38,124,125]. TBI-induced upregulation of vWF expression is mainly considered a marker of endothelial damage[126]. However, it also represents a pro-coagulation compensatory mechanism protecting clotting factor VIII from proteolysis [57,127]. Noticeably, vWF was alsoexpressed in the brain of NHCY-CCI rats and was exacerbated in HHCY-CCI rat brains, suggesting HHCY influence on vWF expression. Although the mechanism is not fully understood, increased vWF expression in HHCY-sham rats, which is exacerbated in HHCY-CCI rats, may result from its pro- coagulant properties aiming to counteract microbleeding associated with the injurious effects of HHCY [19]. In addition to HHCY-induced exacerbation of vWF levels in CCI-rat brains, HHCY also stimulated the increase of blood clotting factor 2a, thrombin, in the plasma of both sham and CCI rats. Several reports have linked HHCY to thrombosis, and increased thrombin generation in hyperhomocysteinemic patients with HHCY was considered the putative mechanism[128,129]. Thrombotic properties of HCY are associated with increased oxidative stress and the secretion of pro-inflammatory molecules[130–132]. These findings indicate that HHCY-induced increased thrombin expression represents an independent risk factor for arterial or deep vein thrombosis and can be viewed as a post-trauma complication.

Inflammatory response after TBI is another important pathological event that leads to the surge of pro-inflammatory molecule production followed by increased expression of cell adhesion molecules onthe surface of cerebrovascular endothelium, causing a flux of inflammatory cells from circulating blood into the brain parenchyma [133–135]. Our study found a profuse presence of the cell adhesion molecule ICAM-1 around the impact region of NHCY-CCI rats' brain, which was exacerbated by HHCY, leading totheir presence in other brain regions such as the somatosensory-2 cortex not found or scarcely present in NHCY-CCI brains. In addition, ICAM-1 was also expressed along cerebral blood vessels of HHCY- sham rats. A previous report by Kamat and colleagues [120] showed increased ICAM-1 expression in the brain of mice intracerebrally injected with HCY. In another study, the harmful effect of HHCY in cystathionine beta-synthase deficient mice led to increasing leukocyte adhesion molecules on activated blood vessel endothelium [19]. Similar to the expression pattern of ICAM-1, CD-68 positive cells, a markerof activated microglia and macrophages demonstrating a diffuse presence of inflammatory cells in the cortex of HHCY rats, which may be mediated by HHCY-induced increase in ICAM-1 levels. The intensecortical association of the detrimental impact of HHCY on TBI pathophysiology, including BBB and inflammation, contributed to HHCY worsening TBI-induced lesion volume in CCI-rat brains. HHCY was previously shown to exacerbate injury lesions in a rodent model of global ischemia [20]. The multitude of TBI associated pathological markers altered by HHCY in this study have a profound influence on corticalbrain regions such as the prefrontal and the parietal cortex that mediate anxiety-like behaviors [69–71], andconsistent with the worsening of the mTBI we observed with brain-injured hyperhomocysteinemia rats that exhibited greater anxiety-like behaviors than CCI alone or sham controls.

In summary, our results demonstrated that moderate HHCY increased oxidative stress as indicated by elevated lipid peroxidation and oxidative nitric oxide in brain regions far beyond the impact area in this mild TBI model. This physiological stress condition enhanced the expression of blood clottingpromoting proteins and worsened TBI-associated blood-brain barrier damage. This happened via the alteration of tight junction protein expression and endothelial dysfunction, which we conjecture leads to the diffuse presence of inflammatory cells in diverse cortical regions, including the corpus callosum andthe somatosensory 2-cortex. Furthermore, HCY accumulation worsened TBI-induced lesion volume and overall increased anxiety-like behavior. These data suggest that monitoring and mitigating HHCY in TBIpatients may prove therapeutically valuable, and we are developing animal models to test specific therapeutic targets for the management of HHCY in mTBI.

4.3 Hyperomocysteinemia and hippocampal vulnerability following mild TBI in rats

Traumatic brain injury interpatient pathological variability represents a challenge for developing an effective therapeutic agent. Mild-TBI represents more than 80% of all TBI cases, with the condition usually resolving within weeks. However, 15-30% of victims suffer long-lasting mTBI related pathologicaland behavioral sequela[136,137]. There is presently no way to determine which individuals may be susceptible to the long-lasting sequela of mTBI pathologies. One candidate we have been investigating is HHCY (HHCY), the neurotoxic accumulation of the non-proteinogenic amino acid HCY. We recently reported on the detrimental effects of HHCY on mTBI pathological outcomes in rat cortex in a controlledcortical impact model[33]. Since HCY and HHCY conditions occur throughout the brain, we hypothesized that there could be additive effects of HHCY in brain regions not directly part of the cortical impact, i.e., the hippocampus.

HHCY can occur in diverse stressful situations, including those sustained by U.S active-duty members on the battlefield or during 'routine' deployments to regions of potential conflict[9]. HHCY neurotoxic properties include its ability to act as a potent agonist to NMDA receptors[17,18,138], which are highly expressed in the dentate gyrus of the hippocampus [139,140]. Thus, a large population of soldiers at risk of mTBI from conflict are also subject to chronic stressors which lead to HHCY. Therefore, we investigated HHCY impact on mTBI-associated neuropathology on the hippocampal dentate gyrus, responsible for several brain-associated memory functions, including hippocampus-dependent working memory[141,142]. Our results present novel findings showing additive harmful effects of HHCY on mTBI- associated oxidative stress, blood-brain barrier dysfunction, neuronal cell loss, and related molecular mechanisms in the rat hippocampus. We also found that the overall impact of these neuropathological changes decreased hippocampus-dependent working memory working performance.

Oxidative stress following TBI is an important marker of the injury pathological progression because it promotes reactive chemical species production and mediates several TBI-associated pathophysiological events, including BBB damage and cell death[38,143–145]. HHCY has been shown to trigger nitrotyrosine expression by suppressing the expression of dimethylarginine- dimethylaminohydrolase and causing the ADMA, an inhibitor of nitric oxide synthase. This subsequently causes increased nitrotyrosine formation from peroxynitrite. Our results showed that the combination of HHCY and mTBI-induced oxidative stress aggravated the expression of 3-nitrotyrosine in the hippocampal DG of HHCY-CCI-rats. Due to its stress-inducing effects, elevated HCY has been shown to promote the death of neuronal precursor cells via multiple cell death mechanisms, including apoptosis and autophagy[146,147]. The hippocampal DG sub-granular zone is one of the two areas of the central nervous system where adult neurogenesis occurs, forming replacement DG granule cells[148] that are functionally integrated into the hippocampal circuit[149,150]. This may make the DG particularly sensitive to the neurotoxicity of HHCY. However, we have also shown significant HHCY induced toxicity exacerbation of cortical injury[33], a region not associated with neurogenesis, suggesting this neurotoxicity of HHCY is widespread.

The blood-brain barrier is a neurovascular unit that regulates the movement of substances and blood-borne immune cells into the brain parenchyma[151]. Therefore, changes to the molecular and cellular components of the BBB can result in an increased presence of neurotoxins, pro-inflammatory cells, and other molecules in the brain parenchyma that could alter brain function or disease progression. Our assessment of the effects of HHCY on TBI-associated BBB dysfunction found that although mTBI alone had a small but significant impact on decreasing the expression of a major tight junction protein occludin. However, the combination of mTBI and HHCY had a more substantial impact and reduced occludin expression on days 1 and 7 after injury. Moreover, the combination of mTBI and HHCY also caused significant enlargement and elongation of endothelial cells nucleus, suggesting structural and molecular perturbations of the blood-brain barrier are occurring consistent with HHCY blood-brain barrier leaking previously reported with this condition[33,84]. The detrimental effects of HHCY on BBB disruption in the hippocampus may be associated with its ability to induce oxidative stress, which is also known to mediate BBB breakdown. Indeed, we showed that HHCY and mTBI significantly disrupt blood-brain barrier integrity in the cerebral cortex following CCI elevating Evans's blue extravasation[33]. Kamat and colleagues (2006) also reported increased Evans blue extravasation in cystathionine beta-synthase deficient-hyperhomocysteinemic mice[84]. Furthermore, the effect of HHCY on BBB permeability may result from HCY's ability to cause vascular microbleeding associated with vascular injuries[152]. The hippocampusvascular architecture composed of several transverse and longitudinal arteries and veins, as represented in the hippocampal fissure (Figure 2C), indicates that BBB disruption in the hippocampal fissure may cause a profuse release of unwanted and potentially toxic substances in the hippocampus.

HCY neurotoxic cell death is attributed to its ability to cause DNA fragmentation, resulting in cell death-inducing poly-ADP-ribose polymerase (PARP) or caspase activation[18]. HCY has also been shownto cause cell death by acting as a potent analog of NMDA receptors, causing excitotoxic apoptotic cell death[17,18,138]. In this study, we assessed the effects of HHCY on other pro-apoptotic cell death mediators, including BAX, a member of the BCL2 protein family, and α-ii spectrin proteolysis. The combination of HHCY and mTBI increased BAX expression and α-ii spectrin proteolysis in the rat hippocampal tissues. Although HHCY-induced BAX increased expression was observed on days 1 and 7 post-injury, increasedα-ii spectrin breakdown products were observed on day 7 post-surgery. This suggests that α-ii spectrin proteolysis is a delayed process preceded by other apoptotic-inducing proteins such as BAX and cleaved caspase. Notably, changes in 145-150 kdal fragments of α-ii spectrin breakdown products are mostly reported following TBI[153–155]. In this study, changes in α-ii spectrin proteolytic breakdown occur with the breakdown products at 100 and 70-45 kdal, suggesting a brain region-specific breakdown pattern. Previous studies reported that HCY intracerebroventricular injection to the rat brain or in vitro treatment of human endothelial cells with HCY upregulated BAX expression[156]. Conversely to cell death signaling pathways activated under neurodegenerative conditions, cell survival-promoting proteins such as ERK1/2 and AKT are required under normal homeostasis conditions to promote cell survival through theirprotective effects on the brain-derived neurotrophic factor[157]. However, in several other neuropathologicalconditions, including TBI, their activation is suppressed in parallel with activated pro-apoptotic markers[32,42] to promote brain cell loss. In our experiment, HHCY alone reduced AKT phosphorylation in sham rats, which was exacerbated in HHCY-CCI rats. AKT phosphorylation was also upregulated in thehippocampus of NHCY-CCI rats on day 1 post-injury before returning normal on day 7. HHCY had similareffects on ERK phosphorylation. These results suggest that, while restoring ERK and AKT phosphorylation on day 7 post-injury in NHCY-CCI suggests at least a progressive recovery from CCI- induced brain injury, the further reduction in HHCY-CCI rats could be indicative of an active progressionof the TBI pathology process.

Brain cell death following CCI-induced mTBI is typically confined to the impact site of the ipsilateral hemisphere, logically as pathology primarily ipsilateral is one of the conditions used to define mild TBI. Our study here on the hippocampus is consistent with that classification, showing in sham animals relatively little neuronal cell loss on the contralateral hippocampus with the mTBI we induced. However,we found a

significant increase in neuronal cell loss in both the ipsilateral and contralateral dentate gyrusof HHCY-sham rats. Noticeably, the combination of HHCY and mTBI caused a dramatic reduction in neuronal density in the contralateral dentate gyrus that was as significant as the neuronal loss in the ipsilateral side where the CCI impact event occurred. These results suggest that, while CCI-induced mTBI mainly impacts the ipsilateral brain hemisphere, HHCY has a systemic effect in both hemispheres. One possibility is that HHCY primes cells in the contralateral dentate gyrus, making them more vulnerable andprone to death after mTBI and/or conversely, the stresses occurring with mTBI render the cells vulnerableto HHCY induced loss of neurons. In either case, the combination of mTBI and HHCY dramatically extends the area of injury risk in the brain. Regions such as the contralateral hemisphere that would not typically exhibit neuronal loss with mTBI, now indicate significant injury when HHCY is present with the mTBI.

The hippocampus is the epicenter of memory and cognition in humans and many animal species[158,159]. Therefore, the cumulative detrimental impact of HHCY on several TBI pathologicalmarkers, resulting in increased hippocampal neuronal cell loss, may affect hippocampus-associated behavioral functions. Consistently, the Y maze test found significant deficits in the hippocampus- dependent working memory performance in HHCY-CCI rats on days 1 and 7 post-injury, compared to NHCY-sham controls. Although HHCY-CCI rats showed improvement in working memory performanceafter that, they still maintained at least a 15% deficit up to day 28 post-injury compared to animals in otherexperimental groups. In agreement with our observation, prior studies reported that HHCY exacerbatedmemory deficits in other neurological disorders, including stroke and Alzheimer's disease[160,161].

4.4 Chronic psychological stress and pathophysiological outcomes of mild TBI in rats

Stress can be triggered by numerous extrinsic or intrinsic stimuli that cause substantial biochemical and physiological changes. In response to a stressful event, our body activates several mediatory pathways, primarily aiming to mitigate the impact of stress-induced biochemical changes on various organs, including the brain. For example, the hypothalamic-pituitary-adrenal (HPA) axis is the primary mediator of stress[162] (Figure 1). HPA axis is activated after stress exposure, leading to increased glucocorticoid secretion contributing to maintaining homeostasis in a fight or flight adaptive response paradigm[163,164]**.** Inparallel, increased homocysteine (HCY), a non-proteinogenic amino acid, is another critical physiologicalresponse to stress exposure[13,14,165]. Like the fight or flight adaptive response to stress, acute stress facilitates HCY transsulfuration to promote the downstream formation of the antioxidant glutathione andattenuate free radical formation[166]. However, chronic stress exposure results in systemic physiological and biochemical changes leading to a sustained increase in glucocorticoid production[167] and HCY accumulation[13] that causes an allostatic overload associated with neurotoxicity and damage that contribute to the onset of several neuropsychiatric disorders[168,169]. This chronic stress-induced allostaticoverload mainly impacts certain brain regions, including the hippocampus (HP), PFC, and amygdala[170–172]. These are associated with behavioral alterations such as increased anxiety, cognitive impairments, decreased motor activity, and sleep dysfunction[172,173]. At the molecular level, a sustained increase of glucocorticoids or HCY increases oxidative stress[115,146,174–176] triggers pathologicalevents such as inflammation and BBB disruption, involved in the pathological progression of several neurological disorders, including TBI. Molecular signaling mechanisms involved in that process include the matrix metalloproteinase-9 activation-induced BBB disruption[111,177], and NFk-B activation[178] of inflammatory cells and associated molecules such as cytokines, chemokines, and adhesion molecules[133–135,179–181.] This event also potentiates oxidative damage, increases neurotoxicity or excitotoxicity, and results in cell death[111,182,183] (Figure 1). The cell death pathway involves HCY or glucocorticoid's ability to stimulate glutamate secretion that binds to N-methyl-D-aspartate (NMDA) and trigger the excitotoxic flux of intracellular calcium that causes the increased generation of reactive oxygenspecies[184]. Moreover, HCY can also cause excitotoxicity by acting as a potent agonist of NMDA receptor[17,138,185].

Sanchez and colleagues recently reported on the effects of earlier life stress (ELS) on TBI occurring later in life. They found that the combination of early life stress induced by separating Sprague Dawley pups from their nursing mother, with TBI sustained by the pups in adulthood, impaired hippocampal-dependent learning, and spatial working memory associated with cortical atrophy. Those findings were associated with increased corticosterone levels[186]. Following the advent of the Iraq and Afghanistan wars, stress paradigms related to military exposure to explosive blasts drew some investigators who studied their impact in TBI models. In that respect, Kwon and colleagues examined the effect of combined predator and unpredictable stressors on explosive blast overpressure induced brain injury in rats. They found increased serum corticosterone levels, inflammation markers, and cell death than in non-stressed blast rats[187]. They also observed lasting behavioral impairments following intermittent exposure of TBI rats tostressors[187]. In another study, post-injury foot shock stress to mice subjected to repeated concussive TBIworsened cognitive impairments and depressive-like behaviors[188].

In summary, Restraint-induced chronic psychological stress significantly increased plasma HCY concentration and elevated oxidative stress markers 4-HNE and MDA. Besides, it worsened TBI induced decreased expression of ZO-1 and occludin, resulting in systemic inflammation resulting in a dense presence of activated inflammatory cells microglia/macrophages in brain regions far beyond the impact site, including the somatosensory cortex. Chronic psychological stress also worsened mTBI-induced impairments of anxiety-like behavior, fine motor activity and caused delayed deficits in hippocampus-dependent working memory.

5.0 CONCLUSIONS AND WAY FORWARD

This study demonstrated that stressful conditions sustained by U.S service members on the battlefield or during aeromedical evacuation increase oxidative stress and alter HCY metabolism. Duringthese combat-related stressful conditions, hypobaria-induced stress facilitates HCY transsulfuration to promote a compensatory increased formation of glutathione, a potent antioxidant to mitigate free radicalformation. Unlike hypobaria, chronic psychological stress causes HCY accumulation, resulting in HHCYin 50-60% of chronically stressed animals and we demonstrated that HHCY exacerbates mild TBI- associated cortical and hippocampal pathological outcomes.

Overall, our findings elucidated TBI-related pathological markers exacerbated by physiological stress and psychological stress sustained by service members. These pathological markers represent therapeutic targets for effective neuroprotective strategies to shield the brain against stress-induced trauma and mitigate combat-related brain injury. Our preliminary results using Omaveloxolone, a broad- spectrum acting therapeutic agent, suggest that it is an outstanding candidate for mitigating the impact of stress on combat-related trauma and effectively manage TBI pathology. Omaveloxolone is proven to attenuate oxidative stress by using synthesized glutathione to detoxify and scavenge free radical formation. It also has anti-inflammatory properties[24,29], can prevent cell death[25,27,28], and attenuate mitochondrial dysfunction. It is pending FDA approval to treat the neurodegenerative disorder Friedreichataxia[23].

This study generated two peer-reviewed publications. A third manuscript cleared by STINFO is submitted for publication and a fourth is being put together on the effects of chronic psychological stress on mild TBI.

Future research should focus on testing the therapeutic potential of Omaveloxolone in the detrimental impacts of stress hypobaria exposure and chronic psychological stress on mTBI pathophysiology.

We anticipate that owing to its broad-spectrum therapeutic action, Omaveloxolone will attenuate several TBI-associated pathological markers and functional hallmarks exacerbated by stress, including oxidative stress, inflammation, cell death, anxiety-like behaviors and working memory deficits. Subsequently, Omaveloxolone will provide an effective and sustained protection against TBI pathology.

6.0 REFERENCES

1 Fang R, Dorlac GR, Allan PF, Dorlac WC. Intercontinental aeromedical evacuation of patients with traumatic brain injuries during Operations Iraqi Freedom and Enduring Freedom. *NeurosurgFocus* 2010; **28**: 1–7.

2 Goodman MD, Makley AT, Huber NL, Clarke CN, Friend LAW, Schuster RM *et al.* Hypobaric hypoxia exacerbates the neuroinflammatory response to traumatic brain injury. *J Surg Res* 2011.doi:10.1016/j.jss.2010.05.055.

3 Skovira JW, Kabadi S V., Wu J, Zhao Z, Dubose J, Rosenthal R *et al.* Simulated Aeromedical Evacuation Exacerbates Experimental Brain Injury. *J Neurotrauma* 2016. doi:10.1089/neu.2015.4189.

4 Proctor JL, Mello KT, Fang R, Puche AC, Rosenthal RE, Fourney WL *et al.* Aeromedical evacuation-relevant hypobaria worsens axonal and neurologic injury in rats after underbody blast-induced hyperacceleration. *J Trauma Acute Care Surg* 2017. doi:10.1097/TA.0000000000001478.

5 Siervo M, Riley HL, Fernandez BO, Leckstrom CA, Martin DS, Mitchell K *et al.* Effects of prolonged exposure to hypobaric hypoxia on oxidative stress, inflammation and gluco-insular regulation: The not-so-sweet price for good regulation. *PLoS One* 2014. doi:10.1371/journal.pone.0094915.

6 Effects of deployment on health behaviours in military forces: A review of longitudinal studies.

7 Zamorski MA, Boulos D. The impact of the military mission in afghanistan on mental health in theCanadian Armed Forces: A summary of research findings. *Eur J Psychotraumatol* 2014; **5**. doi:10.3402/EJPT.V5.23822/SUPPL_FILE/ZEPT_A_11814758_SM0001.PDF.

8 O'Callaghan P, Meleady R, Fitzgerald T, Graham I. Smoking and plasma homocysteine. *Eur Heart J* 2002; **23**: 1580–1586.

9 Kade G, Antosiewicz S, Nowak Z, Wankowicz Z. Albuminuria and hyperhomocysteinemia as cardiovascular risk factors in potentially healthy soldiers: A long-term observation. *Med Sci Monit*2012; **18**: CR771-776.

10 Sharma VK, Das SK, Dhar P, Hota KB, Mahapatra BB, Vashishtha V *et al.* Domain specific changes in cognition at high altitude and its correlation with hyperhomocysteinemia. *PLoS One*2014. doi:10.1371/journal.pone.0101448.

11 Effect of chronic alcohol consumption on total plasma homocysteine level in rats - PubMed. https://pubmed.ncbi.nlm.nih.gov/10776661/ (accessed 11 Mar2022).

12 Beulens JWJ, Sierksma A, Schaafsma G, Kok FJ, Struys EA, Jakobs C *et al.* Kinetics of homocysteine metabolism after moderate alcohol consumption. *Alcohol Clin Exp Res* 2005; **29**:739–745.

13 CM S. Plasma homocysteine levels increase in women during psychological stress. *Life Sci* 1999; **64**: 2359–2365.

14 B S, FG de S, V d'Almeida, JN N. Increased homocysteine levels associated with sex and stress in the learned helplessness model of depression. *Pharmacol Biochem Behav* 2004; **77**: 155–161.

15 Tchantchou F, Graves M, Ashline D, Morin A, Pimenta A, Ortiz D *et al.* Increased transcriptionand activity of glutathione synthase in response to deficiencies in folate, vitamin E, and apolipoprotein E. *J Neurosci Res* 2004; **75**: 508–515.

16 Tchantchou F, Graves M, Ortiz D, Rogers E, Shea TB. Dietary supplementation with 3-deaza adenosine, N-acetyl cysteine, and S-adenosyl methionine provide neuroprotection against multiple consequences of vitamin deficiency and oxidative challenge: relevance to age-related neurodegeneration. *Neuromolecular Med* 2004; **6**: 93–103.

17 Deep SN, Mitra S, Rajagopal S, Paul S, Poddar R. GluN2A-NMDA receptor–mediated sustainedCa2+ influx leads to homocysteine-induced neuronal cell death. *J Biol Chem* 2019; **294**: 11154–11165.

18 Kruman II, Culmsee C, Chan SL, Kruman Y, Guo Z, Penix L *et al.* Homocysteine elicits a DNA damage response in neurons that promotes apoptosis and hypersensitivity to excitotoxicity. *J Neurosci* 2000; **20**: 6920–6926.

19 Kamath AF, Chauhan AK, Kisucka J, Dole VS, Loscalzo J, Handy DE *et al.* Elevated levels ofhomocysteine compromise blood-brain barrier integrity in mice. *Blood* 2006; **107**: 591–593.

20 Endres M, Ahmadi M, Kruman I, Biniszkiewicz D, Meisel A, Gertz K. Folate deficiency increasespostischemic brain injury. *Stroke* 2005; **36**: 321–325.

21 Seshadri S, D'Agostino RB, Rosenberg IH, Wilson PWF, Beiser A, Selhub J *et al.* Plasma Homocysteine as a Risk Factor for Dementia and Alzheimer's Disease. *N Engl J Med* 2002. doi:10.1056/nejmoa011613.

22 Jendričko T, Vidović A, Grubišić-Ilić M, Romić Ž, Kovačić Z, Kozarić-Kovačić D. Homocysteineand serum lipids concentration in male war veterans with posttraumatic stress disorder. *Prog Neuropsychopharmacol Biol Psychiatry* 2009; **33**: 134–140.

23 Lynch DR, Chin MP, Delatycki MB, Subramony SH, Corti M, Hoyle JC *et al.* Safety and Efficacyof Omaveloxolone in Friedreich Ataxia (MOXIe Study). *Ann Neurol* 2021; **89**: 212–225.

24 Wei H-J, Pareek TK, Liu Q, Letterio JJ. A unique tolerizing dendritic cell phenotype induced bythe synthetic triterpenoid CDDO-DFPA (RTA-408) is protective against EAE. *Sci Reports 201771* 2017; **7**: 1–13.

25 P H, Z Q, J T, Z X, R L, X J *et al.* RTA-408 Protects Kidney from Ischemia-Reperfusion Injury in Mice via Activating Nrf2 and Downstream GSH Biosynthesis Gene. *Oxid Med Cell Longev* 2017;**2017**. doi:10.1155/2017/7612182.

26 X L, K W, C X, J J, AF C, IH P *et al.* The novel triterpenoid RTA 408 protects human retinal pigment epithelial cells against H2O2-induced cell injury via NF-E2-related factor 2 (Nrf2) activation. *Redox Biol* 2016; **8**: 98–109.

27 Shekh-Ahmad T, Eckel R, Dayalan Naidu S, Higgins M, Yamamoto M, DInkova-Kostova AT *et al.* KEAP1 inhibition is neuroprotective and suppresses the development of epilepsy. *Brain* 2018;**141**: 1390–1403.

28 Abeti R, Baccaro A, Esteras N, Giunti P. Novel Nrf2-Inducer Prevents Mitochondrial Defects andOxidative Stress in Friedreich's Ataxia Models. *Front Cell Neurosci* 2018; **0**: 188.

29 CC Y, CC L, MJ J, LD H, CM Y. RTA 408 Inhibits Interleukin-1β-Induced MMP-9 Expression via Suppressing Protein Kinase-Dependent NF-κB and AP-1 Activation in Rat Brain Astrocytes. *Int JMol Sci* 2019; **20**. doi:10.3390/IJMS20112826.

30 FUKADA S, SHIMADA Y, MORITA T, SUGIYAMA K. Suppression of Methionine-Induced Hyperhomocysteinemia by Glycine and Serine in Rats. *Biosci Biotechnol Biochem* 2006; **70**:2403–2409.

31 Julio-Amilpas A, Montiel T, Soto-Tinoco E, Gerónimo-Olvera C, Massieu L. Protection of

hypoglycemia-induced neuronal death by β-hydroxybutyrate involves the preservation of energylevels and decreased production of reactive oxygen species. *J Cereb Blood Flow Metab* 2015. doi:10.1038/jcbfm.2015.1.

32 Tchantchou F, Puche AA, Leiste U, Fourney W, Blanpied TA, Fiskum G. Rat Model of Brain Injury to Occupants of Vehicles Targeted by Land Mines: Mitigation by Elastomeric Frame Designs. *J Neurotrauma* 2018; **35**: 1192–1203.

33 Tchantchou F, Goodfellow M, Li F, Ramsue L, Miller C, Puche A *et al.* Hyperhomocysteinemia- Induced Oxidative Stress Exacerbates Cortical Traumatic Brain Injury Outcomes in Rats. *Cell Mol Neurobiol* 2020. doi:10.1007/s10571-020-00866-7.

34 Balan IS, Saladino AJ, Aarabi B, Castellani RJ, Wade C, Stein DM *et al.* Cellular alterations inhuman traumatic brain injury: changes in mitochondrial morphology reflect regional levels of injury severity. *J Neurotrauma* 2013; **30**: 367–381.

35 Ramos-Cabrer P, Campos F, Sobrino T, Castillo J. Targeting the ischemic penumbra. In: *Stroke*.2011 doi:10.1161/STROKEAHA.110.596684.

36 Tchantchou F, Xu YN, Wu YJ, Christen Y, Luo Y. EGb 761 enhances adult hippocampal neurogenesis and phosphorylation of CREB in transgenic mouse model of Alzheimer's disease.FASEB J. 2007; **21**: 2400–2408.

37 Tchantchou F, Tucker LB, Fu AH, Bluett RJ, McCabe JT, Patel S *et al.* The fatty acid amide hydrolase inhibitor PF-3845 promotes neuronal survival, attenuates inflammation and improvesfunctional recovery in mice with traumatic brain injury. *Neuropharmacology* 2014; **85**: 427–439.

38 Tchantchou F, Fourney WL, Leiste UH, Vaughan J, Rangghran P, Puche A *et al.* Neuropathology and neurobehavioral alterations in a rat model of traumatic brain injury to occupants of vehicles targeted by underbody blasts. *Exp Neurol* 2017; **289**: 9–20.

39 Tchantchou F, Zhang Y. Selective Inhibition of Alpha/Beta-Hydrolase Domain 6 Attenuates Neurodegeneration, Alleviates Blood Brain Barrier Breakdown, and Improves Functional Recovery in a Mouse Model of Traumatic Brain Injury. *J Neurotrauma* 2013; **30**: 565–579.

40 Scafidi S, Racz J, Hazelton J, McKenna MC, Fiskum G. Neuroprotection by acetyl-L-carnitine after traumatic injury to the immature rat brain. *Dev Neurosci* 2011. doi:10.1159/000323178.

41 Bryan KJ, Lee H, Perry G, Smith MA, Casadesus G. *Transgenic Mouse Models of Alzheimer's Disease: Behavioral Testing and Considerations*. 2009.

42 Tchantchou F, Tucker LB, Fu AH, Bluett RJ, McCabe JT, Patel S *et al.* The fatty acid amide hydrolase inhibitor PF-3845 promotes neuronal survival, attenuates inflammation and improvesfunctional recovery in mice with traumatic brain injury. *Neuropharmacology* 2014; **85**: 427–439.

43 RN H. The value of spontaneous alternation behavior (SAB) as a test of retention in pharmacological investigations of memory. *Neurosci Biobehav Rev* 2004; **28**: 497–505.

44 Mudd SH. Hypermethioninemias of genetic and non-genetic origin: A review. *Am J Med Genet Part C Semin Med Genet* 2011; **157**: 3–32.

45 dos Santos TM, Siebert C, de Oliveira MF, Manfredini V, Wyse ATS. Chronic mild Hyperhomocysteinemia impairs energy metabolism, promotes DNA damage and induces a Nrf2response to oxidative stress in rats brain. *Cell Mol Neurobiol* 2019. doi:10.1007/s10571-019- 00674-8.

46 Rossi R, Dalle-Donne I, Milzani A, Giustarini D. Oxidized forms of glutathione in peripheral bloodas biomarkers of oxidative stress. *Clin Chem* 2006. doi:10.1373/clinchem.2006.067793.

47 Dadas A, Washington J, Diaz-Arrastia R, Janigro D. Biomarkers in traumatic brain injury (TBI): Areview. Neuropsychiatr. Dis. Treat. 2018. doi:10.2147/NDT.S125620.

48 D'Urso G, Mantovani A, Patti S, Toscano E, De Bartolomeis A. Transcranial Direct Current Stimulation in Obsessive-Compulsive Disorder, Posttraumatic Stress Disorder, and Anxiety Disorders. J. ECT. 2018. doi:10.1097/YCT.0000000000000538.

49 Polusny MA, Kehle SM, Nelson NW, Erbes CR, Arbisi PA, Thuras P. Longitudinal effects of mildtraumatic brain injury and posttraumatic stress disorder comorbidity on postdeployment outcomes in national guard soldiers deployed to Iraq. *Arch Gen Psychiatry* 2011. doi:10.1001/archgenpsychiatry.2010.172.

50 Perna AF, Ingrosso D, De Santo NG. Homocysteine and oxidative stress. Amino Acids. 2003. doi:10.1007/s00726-003-0026-8.

51 Cavalca V, Cighetti G, Bamonti F, Loaldi A, Bortone L, Novembrino C *et al.* Oxidative stress andhomocysteine in coronary artery disease. *Clin Chem* 2001.

52 Rodriguez-Rodriguez A, Egea-Guerrero J, Murillo-Cabezas F, Carrillo-Vico A. Oxidative Stress in Traumatic Brain Injury. *Curr Med Chem* 2014. doi:10.2174/09298673216661312171533l0.

53 Khatri N, Thakur M, Pareek V, Kumar S, Sharma S, Datusalia AK. Oxidative Stress: Major Threat in Traumatic Brain Injury. *CNS Neurol Disord - Drug Targets* 2018. doi:10.2174/1871527317666180627120501.

54 Austin RC, Lentz SR, Werstuck GH. Role of hyperhomocysteinemia in endothelial dysfunction and atherothrombotic disease. Cell Death Differ. 2004. doi:10.1038/sj.cdd.4401451.

55 Papatheodorou L, Weiss N. Vascular oxidant stress and inflammation in hyperhomocysteinemia.Antioxidants Redox Signal. 2007. doi:10.1089/ars.2007.1750.

56 Smith NM, Giacci MK, Gough A, Bailey C, McGonigle T, Black AMB *et al.* Inflammation andblood-brain barrier breach remote from the primary injury following neurotrauma. *J Neuroinflammation* 2018. doi:10.1186/s12974-018-1227-0.

57 Lazzari MA, Sanchez-Luceros A, Woods AI, Alberto MF, Meschengieser SS. Von Willebrand factor (VWF) as a risk factor for bleeding and thrombosis. *Hematology* 2012; **17**: s150–s152.

58 Horvath B, Hegedus D, Szapary L, Marton Z, Alexy T, Koltai K *et al.* Measurement of von Willebrand factor as the marker of endothelial dysfunction in vascular diseases. *Exp Clin Cardiol*2004; **9**: 31–34.

59 Garton T, Keep RF, Hua Y, Xi G. Brain iron overload following intracranial haemorrhage. *StrokeVasc Neurol* 2016; **1**: 172–184.

60 De La Ossa NP, Sobrino T, Silva Y, Blanco M, Millán M, Gomis M *et al.* Iron-related brain damage in patients with intracerebral hemorrhage. *Stroke* 2010; **41**: 810–813.

61 Krämer TJ, Sakas W, Jussen D, Krenzlin H, Kempski O, Alessandri B. Thrombin contributes tothe injury development and neurological deficit after acute subdural hemorrhage in rats only in collaboration with additional blood-derived factors. *BMC Neurosci* 2018; **19**: 1–12.

62 Chodobski, Adam, Zink B. *REVIEW: BBB pathophysiology in TBI*. 2012 doi:10.1007/s12975-011-0125-x.Blood-brain.

63 Kumar A, Stoica BA, Sabirzhanov B, Burns MP, Faden AI, Loane DJ. Traumatic brain injury inaged animals increases lesion size and chronically alters microglial/macrophage classical andalternative activation states. *Neurobiol Aging* 2013; **34**: 1397–1411.

64 Sevenich L. Brain-resident microglia and blood-borne macrophages orchestrate central nervoussystem inflammation in neurodegenerative disorders and brain cancer. *Front Immunol* 2018; **9**: 1–16.

65 Mammana S, Fagone P, Cavalli E, Basile MS, Petralia MC, Nicoletti F *et al.* The role of macrophages in neuroinflammatory and neurodegenerative pathways of alzheimer's disease, amyotrophic lateral sclerosis, and multiple sclerosis: Pathogenetic cellular effectors and potential therapeutic targets. *Int J Mol Sci* 2018; **19**: 1–20.

66 Liu Y, Shaw SK, Ma S, Yang L, Luscinskas FW, Parkos CA *et al.* Regulation of leukocyte transmigration: Cell surface interactions and signaling events. Blood. 2011; **172**; **117**: 7; 2284–13; 2295.

67 Lorenzo A Di, Manes TD, Davalos A, Wright PL, Sessa WC. Endothelial reticulon-4B (Nogo-B) regulates ICAM-1-mediated leukocyte transmigration and acute inflammation. Blood. 2011; **117**:2284–2295.

68 Worthylake RA, Burridge K. Leukocyte transendothelial migration: Orchestrating the underlyingmolecular machinery. Curr. Opin. Cell Biol. 2001; **13**: 569–577.

69 de Lima DSC, Francisco E da S, Lima CB, Guedes RCA. Neonatal l-glutamine modulates anxiety-like behavior, cortical spreading depression, and microglial immunoreactivity: analysis indeveloping rats suckled on normal size- and large size litters. *Amino Acids* 2017. doi:10.1007/s00726-016-2365-2.

70 Dehdar K, Mahdidoust S, Salimi M, Gholami-Mahtaj L, Nazari M, Mohammadi S *et al.* Allergen- induced anxiety-like behavior is associated with disruption of medial prefrontal cortex - amygdalacircuit. *Sci Rep* 2019; **9**. doi:10.1038/s41598-019-55539-3.

71 Sang K, Bao C, Xin Y, Hu S, Gao X, Wang Y *et al.* Plastic change of prefrontal cortex mediates anxiety-like behaviors associated with chronic pain in neuropathic rats. *Mol Pain* 2018. doi:10.1177/1744806918783931.

72 Ayala A. Review Article Lipid Peroxidation: Production, Metabolism, and Signaling Mechanisms of Malondialdehyde and 4-Hydroxy-2-Nonenal Antonio. *Med Technol Neurosurg* 2014; **2014**: 9–12.

73 Dalleau S, Baradat M, Guéraud F, Huc L. Cell death and diseases related to oxidative stress:4-hydroxynonenal (HNE) in the balance. *Cell Death Differ 2013 2012* 2013; **20**: 1615–1630.

74 CM S. The lipid peroxidation product 4-hydroxy-2-nonenal: Advances in chemistry and analysis.
Redox Biol 2013; **1**: 145–152.

75 Jang EJ, Kim DH, Lee B, Lee EK, Chung KW, Moon KM *et al.* Activation of proinflammatory signaling by 4-hydroxynonenal-Src adducts in aged kidneys. *Oncotarget* 2016; **7**: 50864.

76 K U, T K. 4-hydroxy-2-nonenal as a COX-2 inducer. *Mol Aspects Med* 2003; **24**: 213–218.

77 Kim CY, Han JS, Suzuki T, Han SS. Indirect indicator of transport stress in hematological valuesin newly acquired cynomolgus monkeys. *J Med Primatol* 2005. doi:10.1111/j.1600-0684.2005.00116.x.

78 McIntosh IB, Swanson V, Power KG, Raeside F, Dempster C. Anxiety and health problems related to air travel. *J Travel Med* 1998. doi:10.1111/j.1708-8305.1998.tb00507.x.

79 Skandsen T, Nilsen TL, Einarsen C, Normann I, McDonagh D, Haberg AK *et al.* Incidence of mildtraumatic brain injury: A prospective hospital, emergency room and general practitioner-based study. *Front Neurol* 2019; **10**. doi:10.3389/fneur.2019.00638.

80 Frost RB, Farrer TJ, Primosch M, Hedges DW. Prevalence of traumatic brain injury in the general adult population: a meta-analysis. *Neuroepidemiology* 2013; **40**: 154–159.

81 Dayani Y, Stierwalt J, White A, Chen Y, Arnaud F, Jefferson MA *et al.* Hypobaria during aeromedical evacuation exacerbates histopathological injury and modifies inflammatory response in rats exposed to blast overpressure injury. *J Trauma Acute Care Surg* 2019. doi:10.1097/TA.0000000000002337.

82 Solleiro-Villavicencio H, Rivas-Arancibia S. Effect of Chronic Oxidative Stress on Neuroinflammatory Response Mediated by CD4+T Cells in Neurodegenerative Diseases. *FrontCell Neurosci* 2018; **12**: 1–13.

83 Cobb CA, Cole MP. Oxidative and nitrative stress in neurodegeneration. Neurobiol. Dis. 2015. doi:10.1016/j.nbd.2015.04.020.

84 Wagner DD, Kamath AF, Chauhan AK, Kisucka J, Dole VS, Loscalzo J *et al.* Elevated levels ofhomocysteine compromise blood-brain barrier integrity in mice. *Blood* 2006; **107**: 591–593.

85 Kamat PK, Mallonee CJ, George AK, Tyagi SC, Tyagi N. Homocysteine, Alcoholism, and Its Potential Epigenetic Mechanism. Alcohol. Clin. Exp. Res. 2016; **40**: 2474–2481.

86 Selhub J. HOMOCYSTEINE METABOLISM. *Annu Rev Nutr* 1999; **19**: 217–246.

87 Miller AL. The methylation, neurotransmitter, and antioxidant connections between folate and depression. *Altern Med Rev* 2008; **13**: 216–226.

88 Tchantchou F. Homocysteine metabolism and various consequences of folate deficiency. *J Alzheimers Dis* 2006; **9**: 421–427.

89 Wright DJ, Renoir T, Smith ZM, Frazier AE, Francis PS, Thorburn DR *et al.* N-Acetylcysteine improves mitochondrial function and ameliorates behavioral deficits in the R6/1 mouse model ofHuntington's disease. *Transl Psychiatry* 2015. doi:10.1038/tp.2014.131.

90 Sandhir R, Sood A, Mehrotra A, Kamboj SS. N-acetylcysteine reverses mitochondrial dysfunctions and behavioral abnormalities in 3-nitropropionic acid-induced Huntington's disease.*Neurodegener Dis* 2012. doi:10.1159/000334273.

91 Hashimoto M, Takenouchi T, Mallory M, Masliah E, Culvenor JG, McLean CA *et al.* The role ofNAC in amyloidogenesis in Alzheimer's disease [2] (multiple letters). Am. J. Pathol. 2000. doi:10.1016/s0002-9440(10)64777-3.

92 Tchantchou F, Graves M, Rogers E, Ortiz D, Shea TB. N-acteyl cysteine alleviates oxidative damage to central nervous system of ApoE-deficient mice following folate and vitamin E-deficiency. *J Alzheimer's Dis* 2005. doi:10.3233/JAD-2005-7206.

93 Karalija A, Novikova LN, Kingham PJ, Wiberg M, Novikov LN. Neuroprotective effects of N-acetyl-cysteine and acetyl-L-carnitine after spinal cord injury in adult rats. *PLoS One* 2012. doi:10.1371/journal.pone.0041086.

94 Eakin K, Baratz-Goldstein R, Pick CG, Zindel O, Balaban CD, Hoffer ME *et al.* Efficacy of N- acetyl cysteine in traumatic brain injury. *PLoS One* 2014. doi:10.1371/journal.pone.0090617.

95 Clark RSB, Empey PE, Bayir H, Rosario BL, Poloyac SM, Kochanek PM *et al.* Phase I randomized clinical trial of N-acetylcysteine in combination with an adjuvant probenecid for treatment of severe traumatic brain injury in children. *PLoS One* 2017. doi:10.1371/journal.pone.0180280.

96 Yang Y, Li L, Hang Q, Fang Y, Dong X, Cao P *et al.* γ-glutamylcysteine exhibits anti-inflammatory effects by increasing cellular glutathione level. *Redox Biol* 2019.

doi:10.1016/j.redox.2018.09.019.

97 Vera M, Torramade-Moix S, Martin-Rodriguez S, Cases A, Cruzado JM, Rivera J *et al.* Antioxidant and anti-inflammatory strategies based on the potentiation of glutathione peroxidaseactivity prevent endothelial dysfunction in chronic kidney disease. *Cell Physiol Biochem* 2018. doi:10.1159/000495540.

98 Power JHT, Blumbergs PC. Cellular glutathione peroxidase in human brain: Cellular distribution, and its potential role in the degradation of Lewy bodies in Parkinson's disease and dementia withLewy bodies. *Acta Neuropathol* 2009. doi:10.1007/s00401-008-0438-3.

99 Kish SJ, Morito CLH, Hornykiewicz O. Brain glutathione peroxidase in neurodegenerative disorders. *Neurochem Pathol* 1986. doi:10.1007/BF02834296.

100 Marchena O de, Guarnieri M, McKhann G. GLUTATHIONE PEROXIDASE LEVELS IN BRAIN. *JNeurochem* 1974. doi:10.1111/j.1471-4159.1974.tb04293.x.

101 Bellinger FP, Bellinger MT, Seale LA, Takemoto AS, Raman A V., Miki T *et al.* Glutathione peroxidase 4 is associated with neuromelanin in substantia nigra and dystrophic axons in putamen of Parkinson's brain. *Mol Neurodegener* 2011. doi:10.1186/1750-1326-6-8.

102 McEwen BS, Nasca C, Gray JD. Stress Effects on Neuronal Structure: Hippocampus, Amygdala, and Prefrontal Cortex. Neuropsychopharmacology. 2016. doi:10.1038/npp.2015.171.

103 McEwen BS, Morrison JH. The Brain on Stress: Vulnerability and Plasticity of the Prefrontal Cortex over the Life Course. Neuron. 2013. doi:10.1016/j.neuron.2013.06.028.

104 Kumar S, Hultman R, Hughes D, Michel N, Katz BM, Dzirasa K. Prefrontal cortex reactivity underlies trait vulnerability to chronic social defeat stress. *Nat Commun* 2014. doi:10.1038/ncomms5537.

105 De Pablos RM, Villarán RF, Argüelles S, Herrera AJ, Venero JL, Ayala A *et al.* Stress increases vulnerability to inflammation in the rat prefrontal cortex. *J Neurosci* 2006. doi:10.1523/JNEUROSCI.0802-06.2006.

106 Geremia E, Baratta D, Zafarana S, Giordano R, Pinizzotto MR, Grazia La Rosa M *et al.* Antioxidant enzymatic systems in neuronal and glial cell-enriched fractions of rat brain during aging. *Neurochem Res* 1990. doi:10.1007/BF00973653.

107 Makar TK, Nedergaard M, Preuss A, Gelbard AS, Perumal AS, Cooper AJL. Vitamin E, Ascorbate, Glutathione, Glutathicne Disulfide, and Enzymes of Glutathione Metabolism in Cultures of Chick Astrocytes and Neurons: Evidence that Astrocytes Play an Important Role in Antioxidative Processes in the Brain. *J Neurochem* 1994. doi:10.1046/j.1471-4159.1994.62010045.x.

108 Schulz JB, Lindenau J, Seyfried J, Dichgans J. Glutathione, oxidative stress and neurodegeneration. Eur. J. Biochem. 2000. doi:10.1046/j.1432-1327.2000.01595.x.

109 Aksenov MY, Tucker HM, Nair P, Aksenova M V., Butterfield DA, Estus S *et al.* The expressionof key oxidative stress-handling genes in different brain regions in Alzheimer's disease. *J Mol Neurosci* 1998. doi:10.1385/JMN:11:2:151.

110 Margulies S, Hicks R, for Traumatic Brain Injury Workshop Leaders CT. Combination therapiesfor traumatic brain injury: prospective considerations. *J Neurotrauma* 2009; **26**: 925–939.

111 Lehner C, Gehwolf R, Tempfer H, Krizbai I, Hennig B, Bauer H-C *et al.* Oxidative Stress and Blood–Brain Barrier Dysfunction Under Particular Consideration of Matrix Metalloproteinases.*Antioxid Redox Signal* 2011; **15**: 1305–1323.

112 Kuriakose M, Younger D, Ravula AR, Alay E, Rama Rao K V., Chandra N. Synergistic Role ofOxidative Stress and Blood-Brain Barrier Permeability as Injury Mechanisms in the Acute Pathophysiology of Blast-induced Neurotrauma. *Sci Rep* 2019; **9**: 1–12.

113 Forrester SJ, Kikuchi DS, Hernandes MS, Xu Q, Griendling KK. Reactive oxygen species in metabolic and inflammatory signaling. *Circ Res* 2018; **122**: 877–902.

114 Cooke JP. Does ADMA cause endothelial dysfunction? *Arterioscler Thromb Vasc Biol* 2000; **20**:2032–7.

115 Tyagi N, Sedoris KC, Steed M, Ovechkin A V, Moshal KS, Tyagi SC. Mechanisms of homocysteine-induced oxidative stress. *Am J Physiol Heart Circ Physiol* 2005; **289**: H2649-56.

116 Lee WC, Wong HY, Chai YY, Shi CW, Amino N, Kikuchi S *et al.* Lipid peroxidation dysregulationin ischemic stroke: Plasma 4-HNE as a potential biomarker? *Biochem Biophys Res Commun* 2012; **425**: 842–847.

117 Ansari MA, Roberts KN, Scheff SW. Oxidative stress and modification of synaptic proteins inhippocampus after traumatic brain injury. *Free Radic Biol Med* 2008; **45**: 443–52.

118 de Boer P, Hoogenboom JP, Giepmans BN. Correlated light and electron microscopy: ultrastructure lights up! *Nat Methods* 2015; **12**: 503–513.

119 Rosenberg GA. Neurological diseases in relation to the blood-brain barrier. *J Cereb Blood FlowMetab* 2012; **32**: 1139–1151.

120 Kamat PK, Kyles P, Kalani A, Tyagi N. Hydrogen Sulfide Ameliorates Homocysteine-Induced Alzheimer's Disease-Like Pathology, Blood-Brain Barrier Disruption, and Synaptic Disorder. *MolNeurobiol* 2016; **53**: 2451–2467.

121 Wang BR, Ou Z, Jiang T, Zhang YD, Zhao HD, Tian YY *et al.* Independent Correlation of SerumHomocysteine with Cerebral Microbleeds in Patients with Acute Ischemic Stroke due to Large- Artery Atherosclerosis. *J Stroke Cerebrovasc Dis* 2016; **25**: 2746–2751.

122 Pirchl M, Ullrich C, Humpel C. Differential effects of short- and long-term hyperhomocysteinaemia on cholinergic neurons, spatial memory and microbleedings in vivo inrats. *Eur J Neurosci* 2010; **32**: 1516–1527.

123 Harris RA, Wang T, Coarfa C, Nagarajan RP, Hong C, Downey SL *et al.* Comparison of sequencing-based methods to profile DNA methylation and identification of monoallelic epigenetic modifications. *Nat Biotechnol* 2010; **28**: 1097–1105.

124 Yokota H, Naoe Y, Nakabayashi M, Unemoto K, Kushimoto S, Kurokawa A *et al.* Cerebral Endothelial Injury in Severe Head Injury: The Significance of Measurements of Serum Thrombomodulin and the von Willebrand Factor. *J Neurotrauma* 2002; **19**: 1007–1015.

125 De Oliveira CO, Reimer AG, Da Rocha AB, Grivicich I, Schneider RF, Roisenberg I *et al.* Plasmavon Willebrand Factor Levels Correlate with Clinical Outcome of Severe Traumatic Brain Injury. *JNeurotrauma* 2007; **24**: 1331–1338.

126 Lip GYH, Blann A. von Willebrand factor: A marker of endothelial dysfunction in vascular disorders? *Cardiovasc Res* 1997; **34**: 255–265.

127 Sadler JE. von Willebrand factor: two sides of a coin. *J Thromb Haemost* 2005; **3**: 1702–9.

128 Undas A, Brozek J, Szczeklik A. Homocysteine and thrombosis: from basic science to clinical evidence. *Thromb Haemost* 2005; **94**: 907–15.

129 Coppola A, Davi G, De Stefano V, Mancini FP, Cerbone AM, Di Minno G. Homocysteine, coagulation, platelet function, and thrombosis. *Semin Thromb Hemost* 2000; **26**: 243–54.

130 Domagała TB, Undas A, Libura M, Szczeklik A. Pathogenesis of vascular disease in hyperhomocysteinaemia. *J Cardiovasc Risk* 1998; **5**: 239–47.

131 Rees MM, Rodgers GM. Homocysteinemia: Association of a metabolic disorder with vascular disease and thrombosis. *Thromb Res* 1993; **71**: 337–359.

132 Lee R, Frenkel EP. Hyperhomocysteinemia and thrombosis. *Hematol Oncol Clin North Am* 2003; **17**: 85–102.

133 Soares HD, Hicks RR, Smith D, McIntosh TK. Inflammatory leukocytic recruitment and diffuse neuronal degeneration are separate pathological processes resulting from traumatic brain injury.*J Neurosci* 1995; **15**: 8223–33.

134 Royo NC, Wahl F, Stutzmann JM. Kinetics of polymorphonuclear neutrophil infiltration after a traumatic brain injury in rat. *Neuroreport* 1999; **10**: 1363–7.

135 Holmin S, Söderlund J, Biberfeld P, Mathiesen T. Intracerebral inflammation after human braincontusion. *Neurosurgery* 1998; **42**: 291–8; discussion 298-9.

136 Mckee AC, Daneshvar DH. The neuropathology of traumatic brain injury. In: *Handbook of Clinical Neurology*. Elsevier B.V., 2015, pp 45–66.

137 Daneshvar DH, Riley DO, Nowinski CJ, McKee AC, Stern RA, Cantu RC. Long-Term Consequences: Effects on Normal Development Profile After Concussion. Phys. Med. Rehabil.Clin. N. Am. 2011; **22**: 683–700.

138 Ho PI, Ortiz D, Rogers E, Shea TB. Multiple aspects of homocysteine neurotoxicity: glutamate excitotoxicity, kinase hyperactivation and DNA damage. *J Neurosci Res* 2002; **70**: 694–702.

139 Doan J, Gardier AM, Tritschler L. Role of adult-born granule cells in the hippocampal functions: Focus on the GluN2B-containing NMDA receptors. *Eur Neuropsychopharmacol* 2019; **29**: 1065–1082.

140 Watanabe Y, Müller MK, von Engelhardt J, Sprengel R, Seeburg PH, Monyer H. Age-DependentDegeneration of Mature Dentate Gyrus Granule Cells Following NMDA Receptor Ablation. *FrontMol Neurosci* 2016; **8**: 87.

141 S B, P V, F G, A G, T W, SE B *et al.* The Human Dentate Gyrus Plays a Necessary Role in Discriminating New Memories. *Curr Biol* 2016; **26**: 2629–2634.

142 T S, VC P, E H, S A, JE L, S L *et al.* Dentate network activity is necessary for spatial working memory by supporting CA3 sharp-wave ripple generation and prospective firing of CA3 neurons.*Nat Neurosci* 2018; **21**: 258–269.

143 Zhang X, Chen Y, Jenkins LW, Kochanek PM, Clark RS. Bench-to-bedside review: Apoptosis/programmed cell death triggered by traumatic brain injury. *Crit Care 2004 91* 2004; **9**:1–10.

144 Sater AP, Rael LT, Tanner AH, Lieser MJ, Acuna DL, Mains CW *et al.* Cell death after traumaticbrain injury: Detrimental role of anoikis in healing. *Clin Chim Acta* 2018; **482**: 149–154.

145 Price L, Wilson C, Grant G. Blood–Brain Barrier Pathophysiology following Traumatic Brain Injury. *Transl Res Trauma Brain Inj* 2016; : 85–96.

146 R O, W H. Mechanisms of homocysteine neurotoxicity in neurodegenerative diseases with special reference to dementia. *FEBS Lett* 2006; **580**: 2994–3005.

147 Wang M, Liang X, Cheng M, Yang L, Liu H, Wang X *et al.* Homocysteine enhances neural stemcell autophagy in in vivo and in vitro model of ischemic stroke. *Cell Death Dis 2019 108* 2019; **10**: 1–14.

148 SM B, S J. Adult neurogenesis: mechanisms and functional significance. *Development* 2014; **141**: 1983–1986.

149 Ramirez-Amaya V, Marrone DF, Gage FH, Worley PF, Barnes CA. Integration of New Neuronsinto Functional Neural Networks. *J Neurosci* 2006; **26**: 12237–12241.

150 Adult-generated neurons in the dentate gyrus send axonal projections to field CA3 and are surrounded by synaptic vesicles - Markakis - 1999 - Journal of Comparative Neurology - Wiley Online Library. https://onlinelibrary.wiley.com/doi/abs/10.1002/%28SICI%291096-9861%2819990419%29406%3A4%3C449%3A%3AAID-CNE3%3E3.0.CO%3B2-I?sid=nlm%3Apubmed (accessed 22 Jul2021).

151 Welcome MO, Mastorakis NE. Stress-induced blood brain barrier disruption: Molecular mechanisms and signaling pathways. *Pharmacol Res* 2020; **157**: 104769.

152 P C. Vascular patterns of the rat hippocampal formation. *Exp Neurol* 1976; **52**: 447–458.

153 ES W, KK W, JG A, ME B, LU N, MC L *et al.* Alpha II-spectrin breakdown products serve as novel markers of brain injury severity in a canine model of hypothermic circulatory arrest. *AnnThorac Surg* 2009; **88**: 543–550.

154 ME S, DF R, LJ D, RR M, KS B, D M *et al.* Alpha II Spectrin breakdown products in immature Sprague Dawley rat hippocampus and cortex after traumatic brain injury. *Brain Res* 2014; **1574**:105–112.

155 Chen S, Shi Q, Zheng S, Luo L, Yuan S, Wang X *et al.* Role of α-II-spectrin breakdown productsin the prediction of the severity and clinical outcome of acute traumatic brain injury. *Exp Ther Med* 2016; **11**: 2049–2053.

156 Ataie A, Ataee R, Mansoury Z, Aghajanpour M. Homocysteine Intracerebroventricular Injection Induces Apoptosis in the Substantia Nigra Cells and Parkinson's Disease LikeBehavior in Rats.*Int J Mol Cell Med* 2013; **2**: 80.

157 K O, H Y, Y D, T T, T F, A T *et al.* Differential activation of extracellular signal-regulated protein kinase in primary afferent neurons regulates brain-derived neurotrophic factor expression after peripheral inflammation and nerve injury. *J Neurosci* 2003; **23**: 4117–4126.

158 LR S. Memory and the hippocampus: a synthesis from findings with rats, monkeys, and humans. *Psychol Rev* 1992; **99**: 195–231.

159 Dusek JA, Eichenbaum H. The hippocampus and memory for orderly stimulus relations. *Proc Natl Acad Sci U S A* 1997; **94**: 7109.

160 Li JG, Praticò D. High levels of homocysteine results in cerebral amyloid angiopathy in mice. *JAlzheimer's Dis* 2014. doi:10.3233/JAD-141101.

161 EM K, SA H, HK E-S, OA S, KA M, EM A *et al.* Cognitive impairment after cerebrovascular stroke: Relationship to vascular risk factors. *Neuropsychiatr Dis Treat* 2009; **5**: 103–116.

162 Cohen S, Janicki-Deverts D, Doyle WJ, Miller GE, Frank E, Rabin BS *et al.* Chronic stress, glucocorticoid receptor resistance, inflammation, and disease risk. *Proc Natl Acad Sci U S A* 2012; **109**: 5995.

163 BS M. Physiology and neurobiology of stress and adaptation: central role of the brain. *Physiol Rev* 2007; **87**: 873–904.

164 ER DK, E V, MS O, M J. Brain corticosteroid receptor balance in health and disease. *Endocr Rev* 1998; **19**: 269–301.

165 FG de S, MD R, S T, JN N, V D. Acute stressor-selective effects on homocysteine metabolism and oxidative stress parameters in female rats. *Pharmacol Biochem Behav* 2006; **85**: 400–407.

166 Tchantchou F, Miller C, Goodfellow M, Puche A, Fiskum G. Hypobaria-Induced Oxidative StressFacilitates Homocysteine Transsulfuration and Promotes Glutathione Oxidation in Rats with MildTraumatic Brain Injury. *J Cent Nerv Syst Dis* 2021; **13**: 117957352098819.

167 Moghaddam B. Stress Preferentially Increases Extraneuronal Levels of Excitatory Amino Acidsin the Prefrontal Cortex: Comparison to Hippocampus and Basal Ganglia. *J Neurochem* 1993; **60**: 1650–1657.

168 Sapolsky RM. Why stress is bad for your brain. Science (80-.). 1996; **273**: 749–750.

169 Ménard C, Pfau ML, Hodes GE, Russo SJ. Immune and Neuroendocrine Mechanisms of Stress Vulnerability and Resilience. *Neuropsychopharmacology* 2017; **42**: 62–80.

170 Tynan RJ, Naicker S, Hinwood M, Nalivaiko E, Buller KM, Pow D V. *et al.* Chronic stress altersthe density and morphology of microglia in a subset of stress-responsive brain regions. *Brain*

Behav Immun 2010; **24**: 1058–1068.

171 Wohleb ES, Hanke ML, Corona AW, Powell ND, Stiner LM, Bailey MT *et al.* β-Adrenergic receptor antagonism prevents anxiety-like behavior and microglial reactivity induced by repeatedsocial defeat. *J Neurosci* 2011; **31**: 6277–6288.

172 Keynejad RC, Frodl T, Kanaan R, Pariante C, Reuber M, Nicholson TR. Stress and functional neurological disorders: Mechanistic insights. *J Neurol Neurosurg Psychiatry* 2019; **90**: 813–821.

173 Chiba S, Numakawa T, Ninomiya M, Richards MC, Wakabayashi C, Kunugi H. Chronic restraint stress causes anxiety- and depression-like behaviors, downregulates glucocorticoid receptor expression, and attenuates glutamate release induced by brain-derived neurotrophic factor in theprefrontal cortex. *Prog Neuro-Psychopharmacology Biol Psychiatry* 2012; **39**: 112–119.

174 JM Y, SJ Y, KN N, C K, R W, EH L. Mechanism of glucocorticoid-induced oxidative stress in rathippocampal slice cultures. *Can J Physiol Pharmacol* 2009; **87**: 440–447.

175 Behl C, Lezoualc'h F, Trapp T, Widmann M, Skutella T, Holsboer F. Glucocorticoids Enhance Oxidative Stress-Induced Cell Death in Hippocampal Neurons in Vitro. *Endocrinology* 1997; **138**:101–106.

176 Liu HH, Shih TS, Huang HR, Huang SC, Lee LH, Huang YC. Plasma homocysteine is associated with increased oxidative stress and antioxidant enzyme activity in welders. *Sci WorldJ* 2013; **2013**. doi:10.1155/2013/370487.

177 E C-J, Y Y, GA R. Diverse roles of matrix metalloproteinases and tissue inhibitors of metalloproteinases in neuroinflammation and cerebral ischemia. *Neuroscience* 2009; **158**: 983–994.

178 Forrester SJ, Kikuchi DS, Hernandes MS, Xu Q, Griendling KK. Reactive Oxygen Species in Metabolic and Inflammatory Signaling. *Circ Res* 2018; **122**: 877–902.

179 S P, Q S, F F, NR B. Redox regulation of glial inflammatory response to lipopolysaccharide andinterferongamma. *J Neurosci Res* 2004; **77**: 540–551.

180 PH C. Reactive oxygen radicals in signaling and damage in the ischemic brain. *J Cereb Blood Flow Metab* 2001; **21**: 2–14.

181 Hsieh HL, Yang CM. Role of redox signaling in neuroinflammation and neurodegenerative diseases. *Biomed Res Int* 2013; **2013**. doi:10.1155/2013/484613.

182 Uttara B, Singh A V., Zamboni P, Mahajan R. Oxidative Stress and Neurodegenerative

Diseases: A Review of Upstream and Downstream Antioxidant Therapeutic Options. *Curr Neuropharmacol* 2009; **7**: 65.

183 Ryter SW, Kim HP, Hoetzel A, Park JW, Nakahira K, Wang X *et al.* Mechanisms of Cell Death inOxidative Stress. *https://home.liebertpub.com/ars* 2006; **9**: 49–89.

184 Lipton P. Ischemic cell death in brain neurons. Physiol. Rev. 1999; **79**: 1431–1568.

185 Poddar R, Paul S. Homocysteine-NMDA receptor-mediated activation of extracellular signal-regulated kinase leads to neuronal cell death. *J Neurochem* 2009; **110**: 1095–1106.

186 Sanchez CM, Titus DJ, Wilson NM, Freund JE, Atkins CM. Early Life Stress Exacerbates Outcome after Traumatic Brain Injury. *J Neurotrauma* 2021; **38**: 555–565.

187 Kwon SKC, Kovesdi E, Gyorgy AB, Wingo D, Kamnaksh A, Walker J *et al.* Stress and traumaticbrain injury: A behavioral, proteomics, and histological study. *Front Neurol* 2011; **MAR**: 1–14.

188 Klemenhagen KC, O'Brien SP, Brody DL. Repetitive Concussive Traumatic Brain Injury Interactswith Post-Injury Foot Shock Stress to Worsen Social and Depression-Like Behavior in Mice. *PLoS One* 2013; **8**: 1–15.

LIST OF SYMBOLS, ABBREVIATIONS AND ACRONYMS

%	Percent
µM	micromolar
µM	micrometer
4-HNE	4-hydroxy-2-nonenal
AE	aeromedical evacuation
AKT,	serine/threonine kinase
BAX,	B-cell CLL/lymphoma 2-associated X protein
BBB	blood-brain barrier
ERK1/2	extracellular signal-regulated kinases 1 and 2
ft	feet
GPx-1	glutathione peroxidase 1
GPx-4	glutathione peroxidase 4
GS	glutathione synthase
GS	glutathione synthase
HCY	homocysteine
Hg	mercury
HHCY	hyperhomocysteinemia
HPA	hypothalamic-pituitary-adrenal
hr	hour
mg/kg	milligram per kilogram
mg/ml	milligram per milliliter
mm	millimeter
mmHg	millimeter mercury
mTBI	Mild traumatic brain injury
nm	nanometer
O2	oxygen
pAKT,	phosphorylated serine/threonine kinase
PBS	Phosphate buffered saline
pERK1/2	phosphorylated extracellular signal-regulated kinases 1 and 2
SPO2	pulse oximetry
TBI	Traumatic brain injury
vWF	Von Willebrand Factor
w/v	weight per volume
ZO-1	Zona occludens
β-actin	Beta actin
ηg/mg	nanogram per milligram
ɣGCL	gamma-glutamyl-cysteine ligase